125962

1044.950207.002

FUSRAP

FUSRAP COMMUNICATIONS DISTRIBUTION
DOE/ORO FORMER SITES RESTORATION DIVISION (EW-93)

DATE PROCESSED BY PDCC 02/03/95

CCN:

FSRD [X] COMM TYPE 1 G T

SAIC SENSITIVE [ ]

COMM REF

ADMIN RCD

SUBJECT TON - Characterization of Soil Samples - Rpt

FROM Rule TO Hart COMM DATE 1/26/95

ADDR CODE NUMBER ST CLOSES CCN WBS 103, 123, 129, 132

SUBJECT CODE 7315 AFFECTED DOCUMENT

RESPONSE TRACKING INFORMATION

ACTION DESCRIPTION:

PRIMARY:	PRIMARY:
OWED TO:	OWED BY: (ORG)
(ORG) TARGET DATE / /	CLOSING CCN COMPL. DATE / / CLOSING REF
SECONDARY:	SECONDARY:
OWED TO:	OWED BY: (ORG)
(ORG) TARGET DATE / /	CLOSING CCN COMPL. DATE / / CLOSING REF

MESSAGE:

[redacted], [redacted] has a copy of the report.

		W/A	W/O			W/A	W/O			W/A	W/O
DIRECTOR, FSRD: [redacted]	FSRD		1	PROGRAM MANAGER: [redacted]	SAIC			PROGRAM MANAGER: [redacted]	BPM		
DEP. DIRECTOR, FSRD:	FSRD			DEPUTY PROGRAM MGR:	SAIC			DEPUTY PROGRAM MGR	BPM		
SITE MANAGER:	FSRD			MGMT. SYSTEMS:	SAIC				BPM		
	FSRD			SECRETARY:	SAIC			PROJECT MANAGER:	BPM		
	FSRD		1						BPM		
	FSRD			[redacted]		1			BPM	1	
	FSRD								BPM		
PROJECT SUPPORT GRP:	FSRD		1				1	COMMUNITY RELATIONS	BCR		
	FSRD						1	CONSTRUCTION	BFC		
	FSRD							ENGINEERING & TECHNOLOGY	BET		
	FSRD							ENGINEERING	BET		
PRGM ANALYST:	FSRD							ENVIR TECH/DATA	BET		
SECRETARY: [redacted]	FSRD							GEOTECH	BET		
FSRD CHRON FILE			1					ENVIRON SAFETY & HEALTH	BEH		
FSRD NOTEBOOKS								SAFETY & HEALTH	BEH		
READING FILE								ENVIR COMPLIANCE	BEH		
DOE/P&CD: [redacted]	DCO							WASTE MGMT & TREATMENT	BEH		
DOE/HQ: [redacted]	DHQ							PROCUREMENT	BPO		
								PROJECT ADMINISTRATION	BPA		
				TMA/EBERLINE	BET			PROJECT AUTOMATION	BAU		
				SITES: 158 NFSS				PROJECT CONTROLS	BPC		
ANL: [redacted]	ANL			TONAWANDA INFO CTR.				TECHNICAL REPORTS	BTR		
[redacted]	ANL			137 WISS				QUALITY ASSURANCE	BQA		
[redacted]	ANL		1	138 MISS/INFO CTR				ADMIN RCD/INFO [illegible]			
[redacted]	ANL			139 COLONIE (CISS)							
ORISE:	ORISE			140 / 153 LATTY AVE/SLAPS				PDCC READ FIL			
ORNL:	ORNL							PDCC: SEN[illegible]			

200.1e

Seaway_01.06_0064_a

ILLUSTRATIONS--Continued

Page

11B. SEM photomicrograph of uranium oxide compounds in slag fragments from 0.3- by 0.15-mm fraction of Seaway bias sample 23
12. SEM photomicrograph of filter cake containing uranium oxide compound 24
13. SEM photomicrograph of clay/carbonate aggregates from the Seaway bias 0.3- by 0.15-mm fraction 24
14. SEM photomicrograph of calcium-uranium carbonate mineral hosted by albite in the Linde/Praxair bias 0.3- by 0.15-mm fraction 25
15. SEM photomicrograph of grain of lead and iron oxides from Ashland 1 bias 0.3- by 0.15-mm fraction 25

TABLES

1. Tonawanda sample description 28
2. Sample weights and moisture contents 28
3. Isotopic analysis of head samples 28
4. Isotopic analysis of sized fractions separated from Ashland 1 samples 29
5. Isotopic analysis of sized fractions separated from Ashland 2 samples 29
6. Isotopic analysis of sized fractions separated from Linde/Praxair samples 30
7. Isotopic analysis of sized fractions separated from Seaway samples 30
8. Isotopic analysis of wash-water samples from sizing procedure 31
9. Particle size analysis, isotope analysis, and distribution for Ashland 1 bias sample 32
10. Particle size analysis, isotope analysis, and distribution for Ashland 1 systematic sample 32
11. Particle size analysis, isotope analysis, and distribution for Ashland 2 bias sample 33
12. Particle size analysis, isotope analysis, and distribution for Ashland 2 systematic sample 33
13. Particle size analysis, isotope analysis, and distribution for Linde/Praxair bias sample 34
14. Particle size analysis, isotope analysis, and distribution for Linde/Praxair systematic sample 34
15. Particle size analysis, isotope analysis, and distribution for Seaway bias sample 35
16. Particle size analysis, isotope analysis, and distribution for Seaway systematic sample 35
17. Results of heavy-liquid separation at specific gravity 2.90 ± 0.02 36
18. Composition, in pct of grain count, of plus 6.4-mm fractions 37
19. Composition, in pct of grain count, of 6.4- by 0.3-mm fractions 37
20. Composition, in pct of grain count, of 0.3- by 0.15-mm fractions 38
21. Composition, in pct of grain count, of 0.15- by 0.075-mm fractions 39

CHARACTERIZATION OF SOIL SAMPLES FROM THE TONAWANDA, NEW YORK SITE

by

A. R. Rule, D. C. Dahlin, and C. A. Summers

EXECUTIVE SUMMARY

The Tonawanda site is composed of the Linde Center (Linde/Praxair), Ashland 1, Ashland 2, and Seaway Industrial Park properties in the industrialized area of Tonawanda, New York. Soils at the four properties are contaminated with low-level radioactivity in the form of thorium (Th-230), uranium (U-238), and radium (Ra-226) and their respective decay products. The Department of Energy (DOE) will decontaminate the properties under its Formerly Utilized Sites Remediation Action Program (FUSRAP).

Eight samples of radiation-contaminated soils from the Tonawanda site were received for characterization studies at the Albany Research Center (ALRC) of the U.S. Bureau of Mines. Each sample is a split of a composite sample of soils collected from multiple locations at each property. The samples are described as "systematic" (average contamination) samples or "bias" (high contamination) samples.

The samples were separated into five size fractions for mineralogical and isotopic analysis . Each sample was attritioned in a blade-type attritioning mill for 5 minutes, and then wet-screened on 6.4-mm, 0.3-mm, 0.15-mm, and 0.075-mm screens. The fines from these soils showed poor to very poor filtering characteristics. Flocculation helped to settle the fines and leave relatively clean supernatant, but the solids filtered very slowly.

Mineralogical and isotopic analyses were completed on representative splits of the sized samples. Samples of wash water were also collected from the sizing step for isotopic analysis. Core Laboratories, Casper, WY, and Controls for Environmental Pollution, Santa Fe, NM, performed the isotopic analyses for thorium, uranium, and radium.

Mineralogical characterization consisted of petrographic-identification and grain-count studies on all but the minus 0.075-mm size fractions, heavy-liquid separation of the 0.3- by 0.15-mm fractions and 0.15- by 0.075-mm fractions, and x-ray diffraction analysis of the minus 0.075-mm size fractions.

Isotopic analyses and material balances show that thorium, uranium, and radium are present in all size fractions at levels well above those acceptable for clean soil. A high percentage of the weight and of the radioactive contaminants is in the finest fractions (minus 0.075 mm).

The soils are mixtures of rocks and mineral grains, natural organic materials (grasses, wood) and man-made materials such as glassy, crystalline, and scoriaceous slags, concrete, plastics, and tramp metals. Radioactive contamination, in the form of uranium compounds, was identified both in man-made materials and in natural ore fragments. The uranium is usually locked in slag, gangue, or other matrix, and, consequently, it occurred in both heavy and light specific-gravity fractions. Thorium was not identified mineralogically, but isotopic analyses confirmed its presence.

Conventional mineral-processing technology is unlikely to produce a significant fraction of clean soil in a volume-reduction strategy. The problem of particle liberation will adversely affect all physical separation techniques. Scrubbing followed by size separation, gravity separation, and magnetic separation would leave significant contamination in all size fractions because unliberated contaminated particles exist in all of the fractions. Selective leaching of these soils to remove contamination would also likely be ineffective.

Based on the information contained in this report, we recommend that DOE-FUSRAP not pursue treatment as an alternative to disposal or long term storage of the contaminated soil at the Tonawanda site.

INTRODUCTION

Description of site

The Tonawanda site is composed of the Linde Center (Linde/Praxair), Ashland 1, Ashland 2, and Seaway Industrial Park properties in the industrialized area of Tonawanda, New York; together these four areas are referred to as the Tonawanda site. Radioactive contamination in the form of thorium (Th-230), uranium (U-238), and radium (Ra-226) and their respective decay products resulted from processing uranium ores under contract with the Manhattan Engineering District (MED) at the Linde property. Subsequent disposal and relocation of the processing residues resulted in contamination of the Ashland 1, Ashland 2, and Seaway properties. The Department of Energy will decontaminate the properties under its Formerly Utilized Sites Remediation Action Program (FUSRAP).[1]

Description of samples in the ALRC study

Eight samples of radiation-contaminated soils from the Tonawanda site were received for characterization studies at the Albany Research Center (ALRC) of the U.S. Bureau of Mines. Each sample is a split of a composite sample prepared by personnel from Bechtel National, Inc., in accordance with a sampling plan from Science Applications International Corp. The samples represent soil collected from multiple locations at each property with a 3-inch auger at depths from 0 to 2 feet below the surface. The samples are described in table 1 as "systematic" (average contamination) samples or "bias" (high contamination) samples.

---

[1]Science Applications International Corp. Tonawanda Site Soil Sampling Plan, 1994.

METHODS

Sample preparation

The procedure used to prepare the samples for mineralogical and isotopic analysis is outlined in figure 1. The as-received samples appeared dry but not dusty, and contained grasses and woody material, as well as minerals and man-made materials. The samples were weighed and then dried at 60°C.[2] To minimize dust in splitting, each dried sample was rolled several times on a rolling cloth to mix and homogenize it. It was then quartered to split a 500-g head sample and two 1-kg test samples for sizing. Originally, it was intended to use a 1-kg sample and hold the other as a reserve, but the sample size requirements for isotopic analysis necessitated using both 1-kg samples.

Size separation

Each 1-kg sample was attritioned in a blade-type attritioning mill for 5 minutes. The first two samples to be treated (3372 and 3376) were attritioned at 65 pct. solids, but these produced very thick slurries that did not allow efficient attritioning. The remaining six samples were attritioned at 50 pct. solids. The primary purposes of attritioning were to break up clumps of soil and clay and to scrub agglomerated fines from coarser particles. The conditions for attritioning were chosen to minimize abrasion of liberated particles, that would have generated additional fines and skewed the size distribution of the soils.

---

[2]U.S. Environmental Protection Agency. Characterization Protocol for Radioactive Contaminated Soils. Publication 9380.1-10FS, 1992.

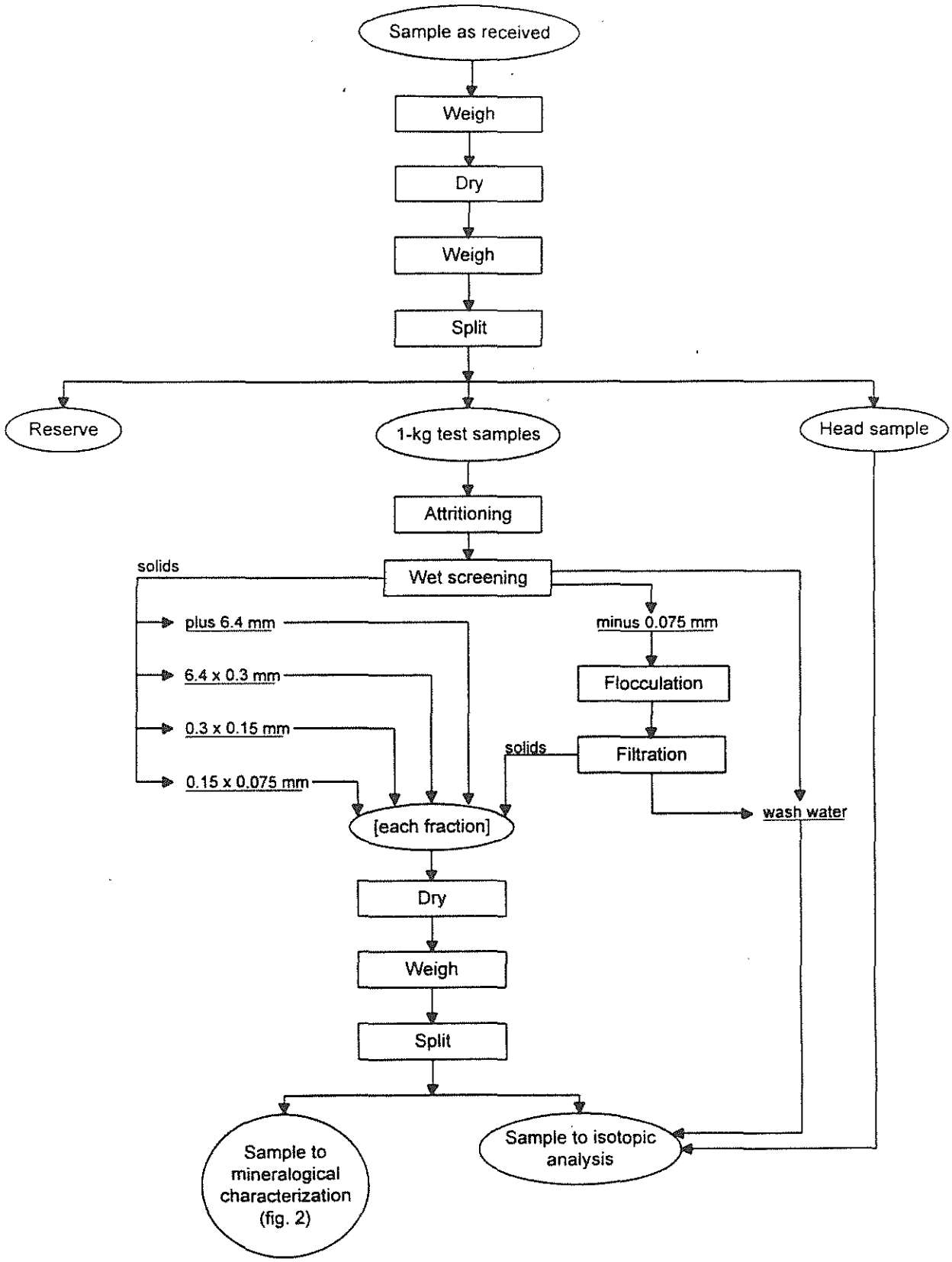

Figure 1. Sample preparation for mineralogical characterization

The attritioned samples were wet-screened on 6.4-mm, 0.3-mm, 0.15-mm, and 0.075-mm screens. Wash water was decanted from the four coarser fractions before they were dried in an oven at 60°C.

A pressure filter, with air pressure at 80 psi, was used to filter all of the minus 0.075-mm fractions. These fractions showed poor to very poor filtering characteristics. To expedite dewatering, a flocculent (Primafloc C-3, Rohm & Haas, Inc.)[3], was used to flocculate the minus 0.075-mm fines. Flocculation helped to settle the fines and leave relatively clean supernatant, but the solids filtered very slowly, even when negligible amounts of solids were on the filter papers. The filter cakes of minus 0.075-mm fines were also dried at 60°C.

Mineralogical and isotopic analyses

After drying, the samples were weighed and prepared for mineralogical and isotopic analyses. The entire plus 6.4-mm fraction was examined for mineralogical content before it was submitted for isotopic analysis; the other size fractions were split, with representative fractions going to mineralogical and isotopic analyses. Samples of wash water were also collected from the sizing step for isotopic analysis.

Two analytical laboratories were utilized for the isotopic analyses. Samples from the Linde/Praxair and Seaway properties (3371 - 3374) were analyzed by Core Laboratories, Casper, WY. The samples from the Ashland 1 and Ashland 2 properties (3375 - 3378) were analyzed by Controls for Environmental Pollution, Santa Fe, NM.

Mineralogical characterization

Mineralogical characterization of the samples followed the procedure outlined in figure 2. The plus 6.4-mm fractions were examined under a binocular microscope to identify and count the constituents. Because most of the sample fractions contained fewer than 100 particles, all of

---

[3]Reference to specific products does not imply endorsement by the Bureau of Mines.

the particles were counted, and the percentages of constituents reported may not be statistically representative of the soil.

The 6.4- by 0.3-mm fractions were also examined under the binocular microscope to identify and count the constituents. Occasionally, single grains were crushed and viewed under a petrographic microscope in refractive-index (RI) oil to confirm identification. Each fraction was thoroughly mixed in its drying pan, and small representative amounts were taken from at least 4 different parts of the sample. The percentages of constituents were estimated in each scoop of material and combined into an estimate for the fraction. Some percentages of constituents may not be statistically representative of this fraction of the soils.

Heavy-liquid separation tests were done on the 0.3- by 0.15- and 0.15- by 0.075-mm size fractions to aid in identifying the constituents. The separation was accomplished using a solution of sodium polytungstate in distilled water at a specific gravity of 2.90 ± 0.02. The petrographic sample split from each size fraction was mixed thoroughly on a rolling cloth and then quartered to get approximately 5 grams of sample. The sample was combined with the heavy liquid in a 50-ml plastic test tube, and the slurry was stirred to ensure complete wetting and mixing. The sample was centrifuged for 5 minutes at 1500 rpm, and then the test tube was dipped in liquid nitrogen to freeze the bottom portion of the heavy liquid that contained the heavy fraction. The light fraction was poured off from the frozen heavy fraction into a Buchner funnel and was thoroughly washed with distilled water. The heavy fraction was thawed, and then filtered and washed the same way as the light fraction. The separated fractions were dried at 60°C, and the recovered polytungstate solution was reused after appropriate adjustment, if necessary, of the specific gravity.

The heavy and light concentrates of the 0.3- by 0.15- and 0.15- by 0.075-mm systematic fractions and the 0.15- by 0.075-mm bias fractions were examined using the binocular and petrographic microscopes. Each light concentrate was split, and small scoops of material from different parts of the split were prepared as grains on glass microscope slides in 1.544 RI oil. A grain count was then completed using the petrographic microscope. The heavy concentrates were separated into magnetic and nonmagnetic portions with a hand magnet, and each was weighed. The magnetic portion of each heavy fraction was examined under the binocular

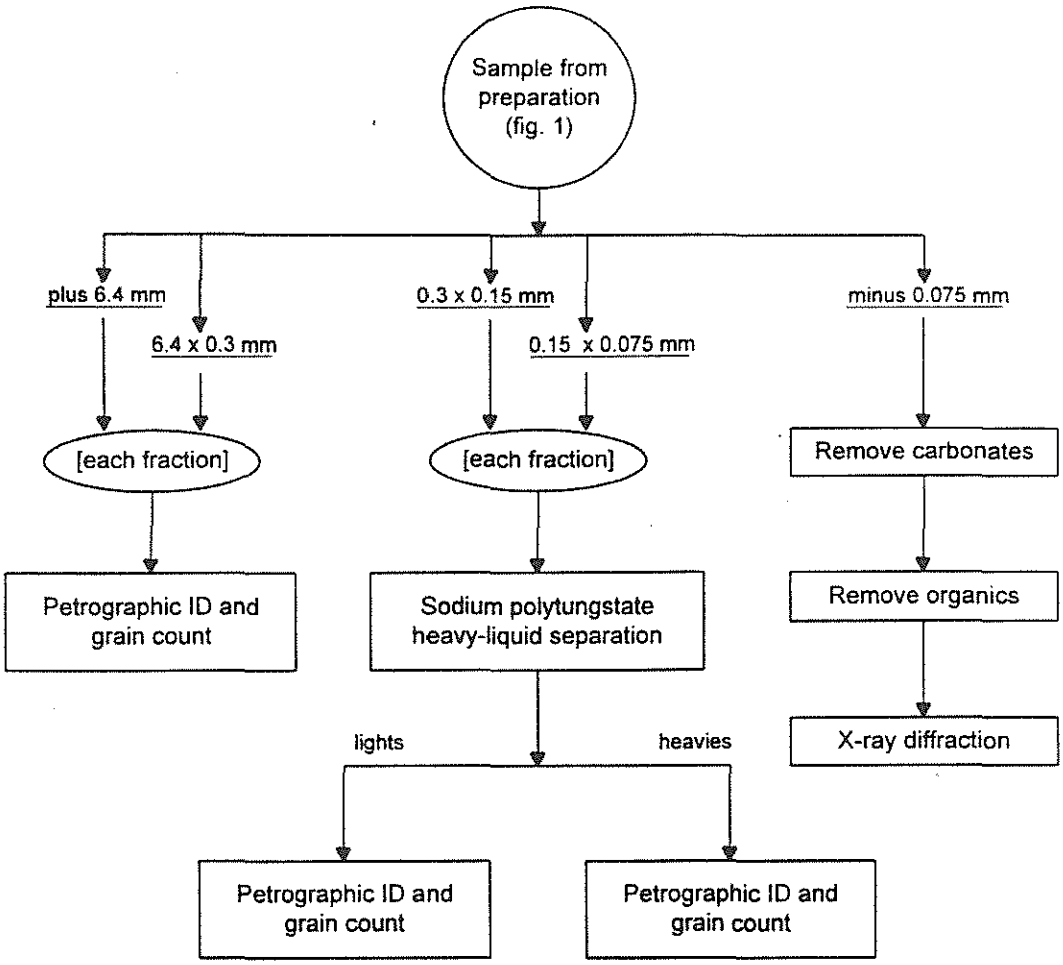

Figure 2. Mineralogical characterization

microscope and its constituents were identified. A few of the nonmagnetic portions were large enough to split, but most were not. Grains from the nonmagnetic portions were prepared in 1.60 RI oil, and grain counts were completed using a petrographic microscope.

The heavy and light concentrates of the bias 0.3- by 0.15-mm fractions were prepared as polished grain mounts. Each of these mounts was examined with a reflected-light microscope and a scanning electron microscope (SEM). Grains were identified by their reflective properties and by their elemental analysis, obtained with energy-dispersive and wavelength-dispersive x-ray analyses (EDX and WDX) from the SEM. All grains in approximately equally spaced multiple fields of view in the SEM were counted as the mount was moved under the electron beam.

The minus 0.075-mm systematic fractions were pretreated for x-ray diffraction studies (XRD) using methods modified from those described by Kunze and Dixon[4]. The pretreatment removed carbonate minerals and organic material to simplify and expedite XRD analyses. A split of each fraction was treated with sodium acetate solution and acetic acid to remove carbonate minerals visible under the petrographic microscope, and then with hydrogen peroxide for removal of organic material. The treated material was submitted for XRD analysis.

RESULTS AND DISCUSSION

Table 2 shows the weights and calculated percent moisture of the samples as received and weights of the dried samples. The percent moisture in the samples was somewhat surprising, given the appearance of the samples. The amount of clays, grasses, and plant materials accounts for the high moisture contents.

---

[4]Kunze, G. W. and J. B. Dixon. "Chapter 5: Pretreatment for Mineralogical Analysis." In Methods of Soil Analysis, Part 1: Physical and Mineralogical Methods, 2nd edition. A. Klute, ed., American Society of Agronomy, Inc., and Soil Science Society of America, Inc., Madison, Wisconsin, 1986.

Radioactivity as a function of size

Isotopic analyses for Th-228, Th-230, Th-232; U-234, U-235, and U-238; and Ra-226 for the eight head samples are shown in table 3, and for the size fractions separated from each sample in tables 4-7. Table 8 shows the isotopic analysis of the wash-water samples taken from the sizing procedures.

Th-230 is noticeably absent from the bias samples and the systematic samples from both Ashland 1 and Ashland 2. The values from the head analyses are confirmed by the analyses of the individual size fractions and the calculated head analyses.

Material balances for the sized fractions are shown in tables 9-16. These data show weight percent, isotope analysis, and isotope distribution for the individual size fractions from each of the eight samples. Calculated heads agree reasonably well with the head analyses for most of the analyses. These results, shown graphically in figures 3-10, indicate that the thorium, uranium, and radium isotopes are present in all size fractions, and that the concentration levels in all size fractions exceed the levels required for classification as clean soil. All of the samples have a high percentage of the weight and the radioactive contaminants in the finest fraction (minus 0.075 mm).

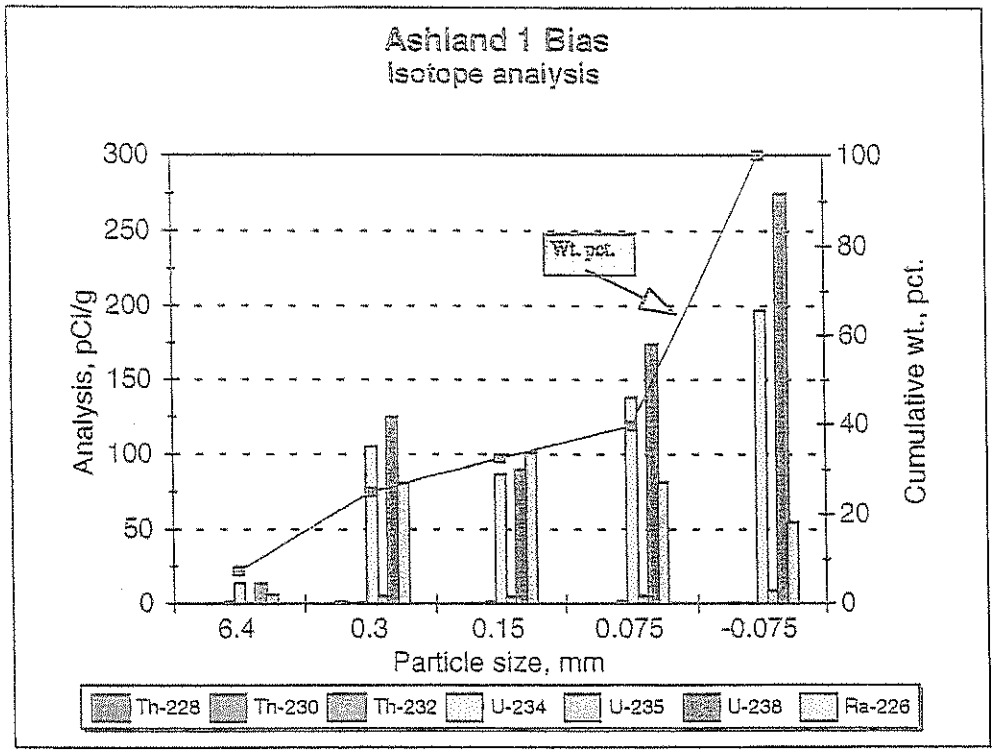

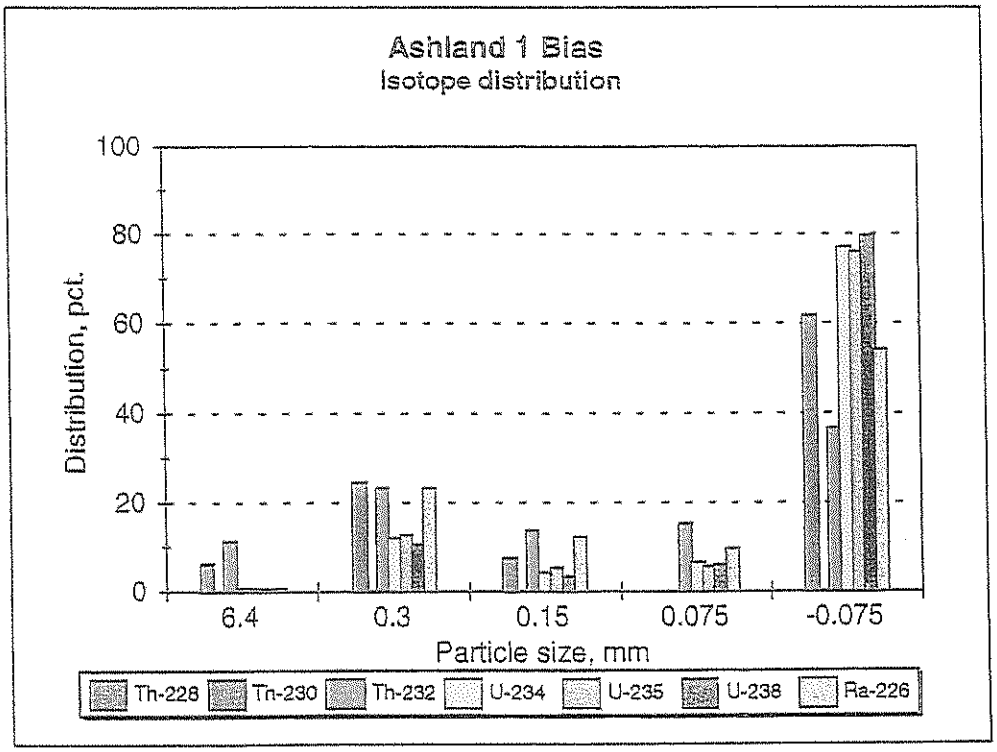

Figure 3. Particle size analysis, isotope analysis, and isotope distribution for Ashland 1 bias sample.

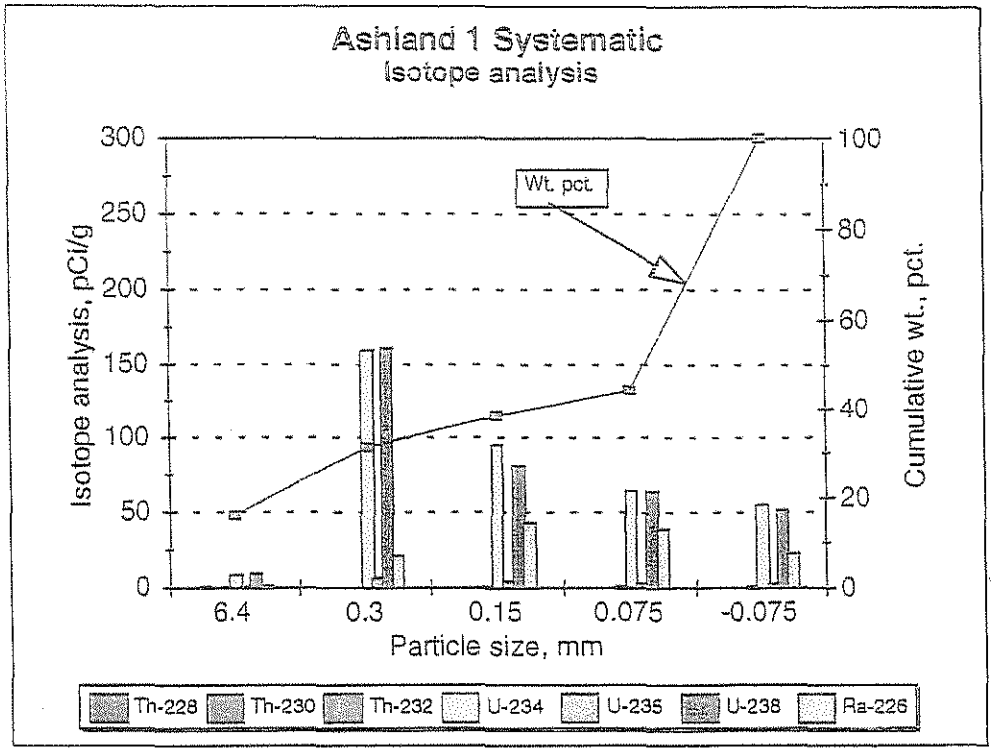

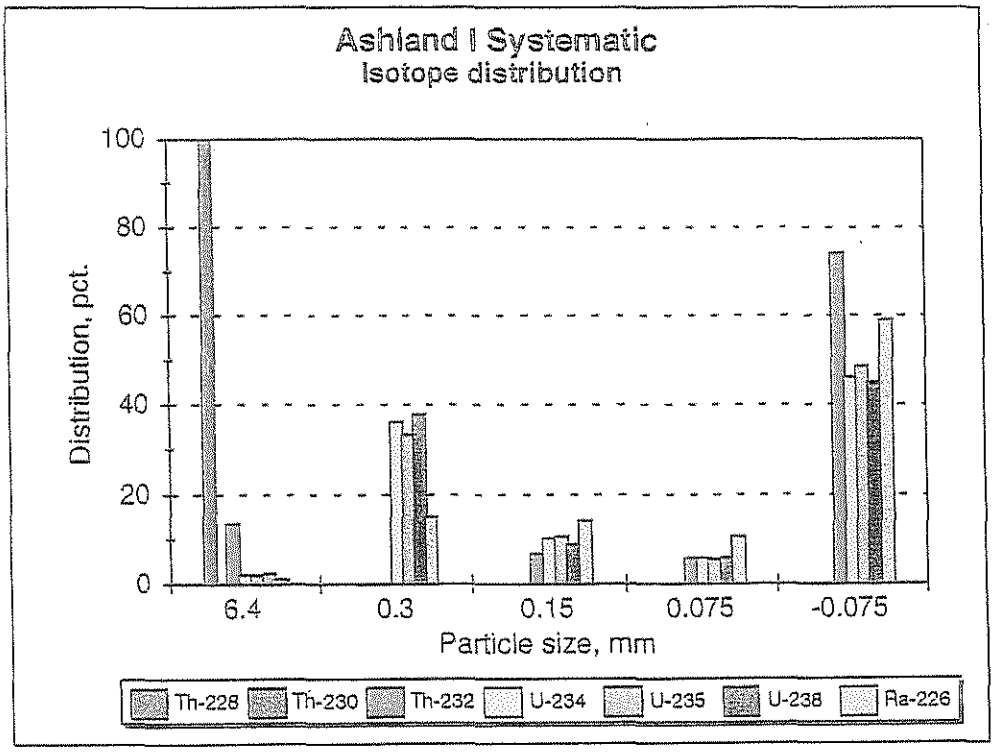

Figure 4. Particle size analysis, isotope analysis, and isotope distribution for Ashland 1 systematic sample.

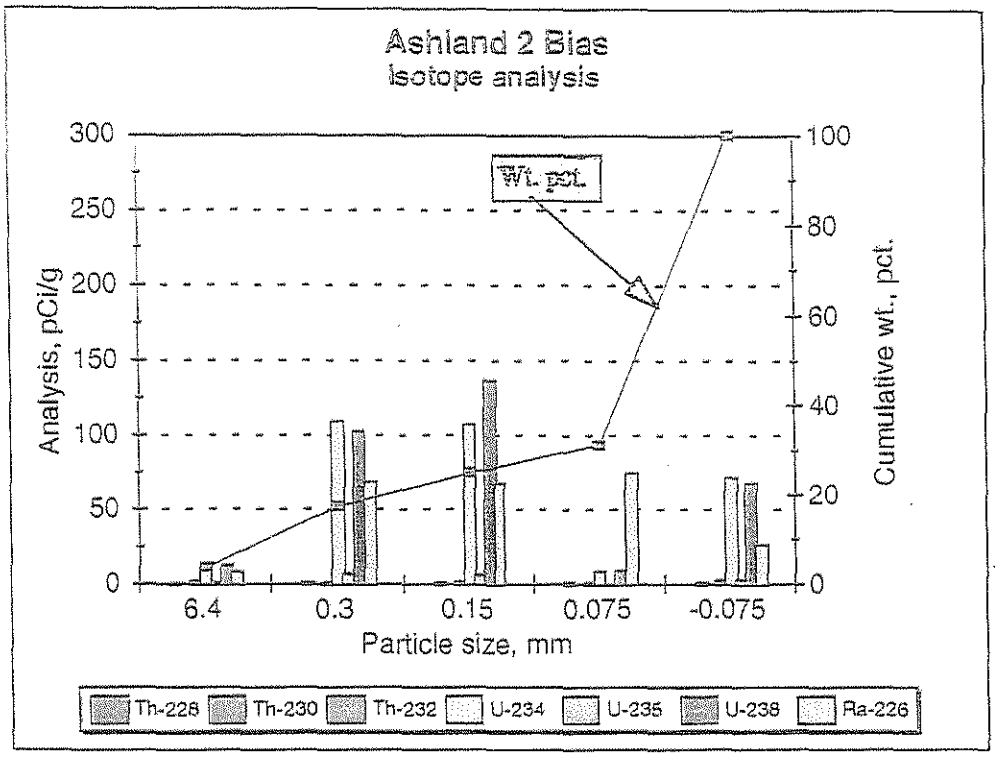

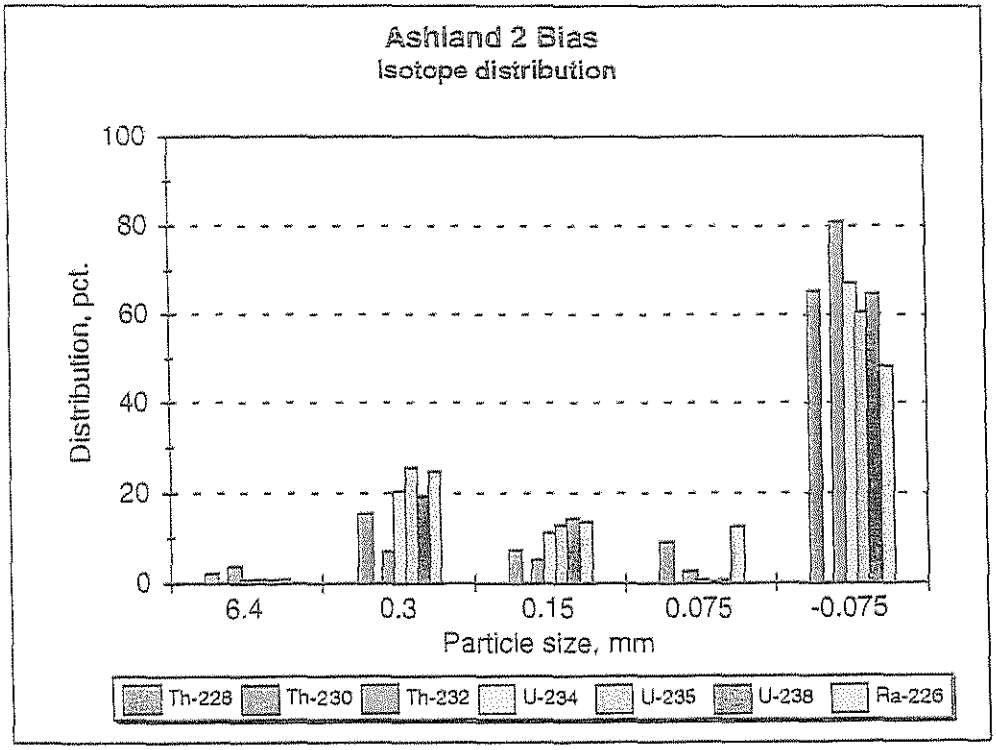

Figure 5. Particle size analysis, isotope analysis, and isotope distribution for Ashland 2 bias sample.

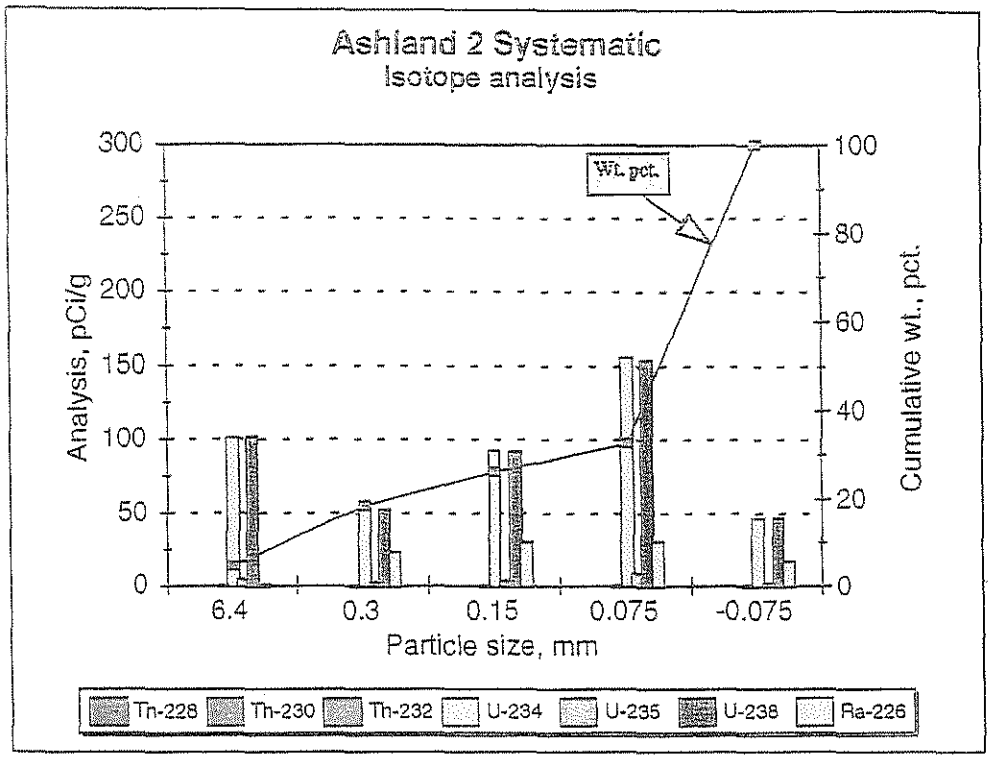

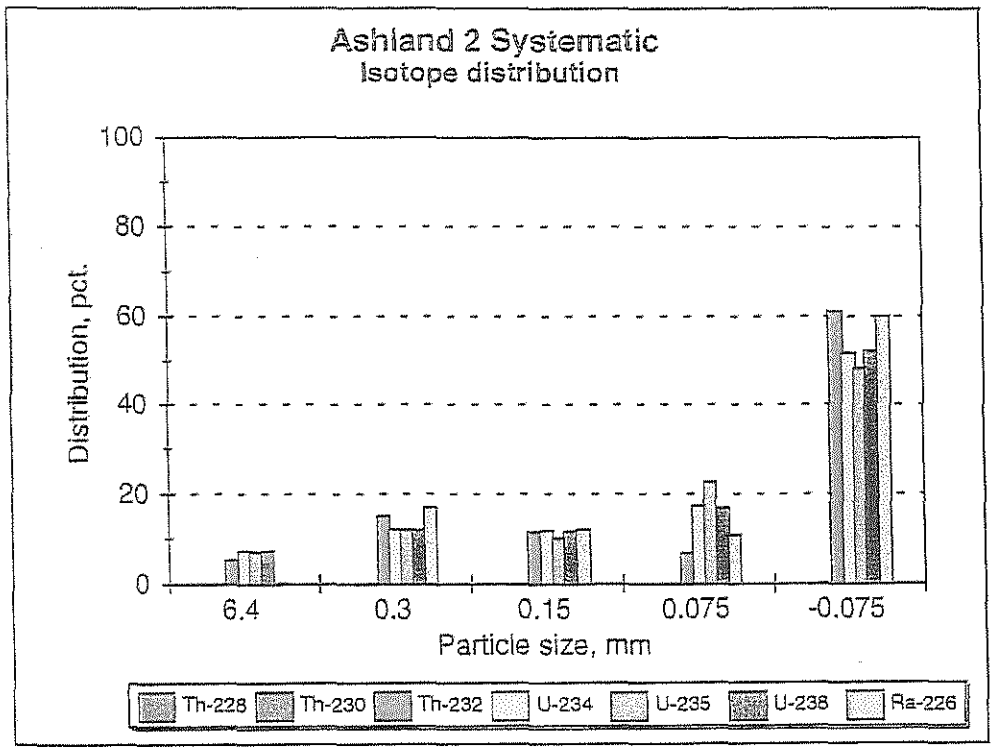

Figure 6. Particle size analysis, isotope analysis, and isotope distribution for Ashland 2 systematic sample.

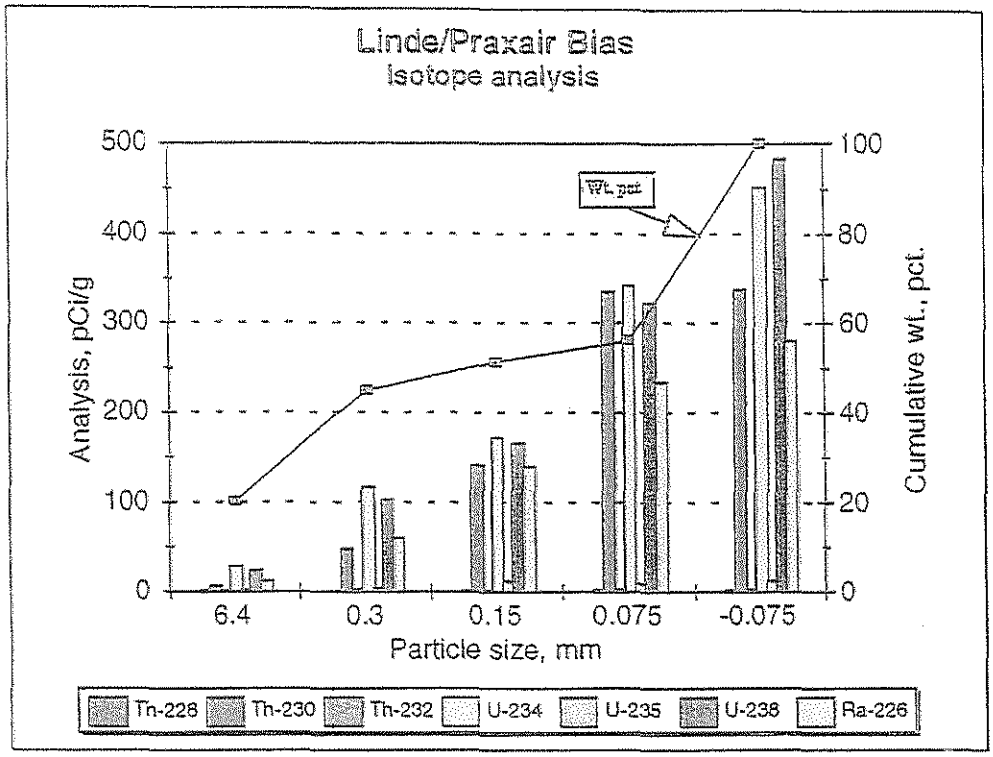

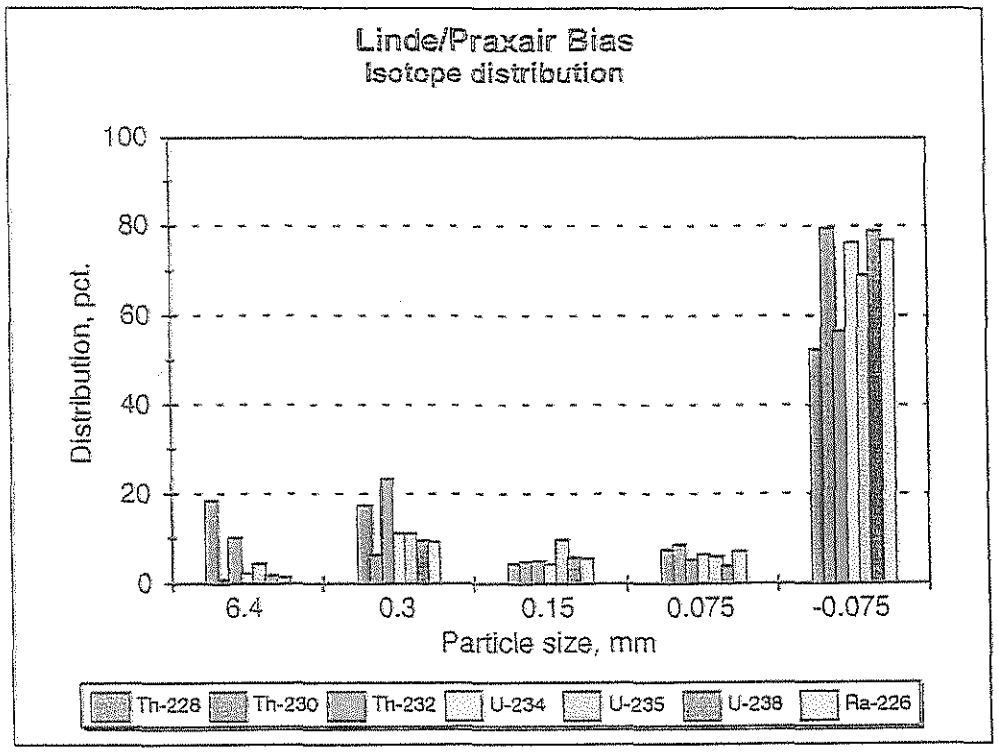

Figure 7. Particle size analysis, isotope analysis, and isotope distribution for Linde/Praxair bias sample.

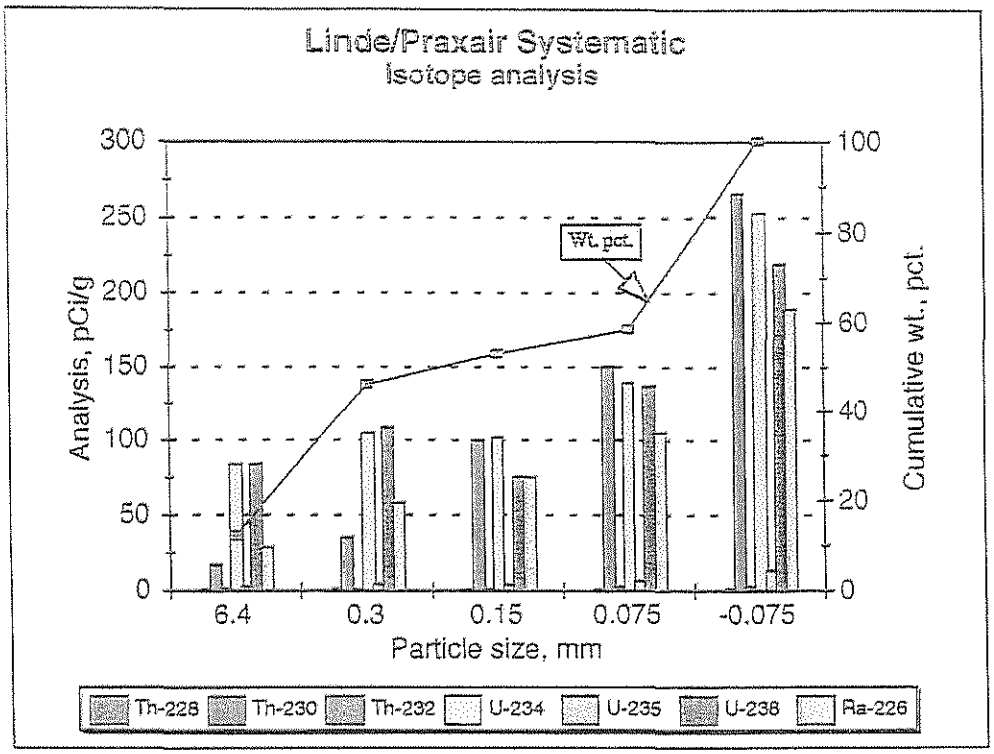

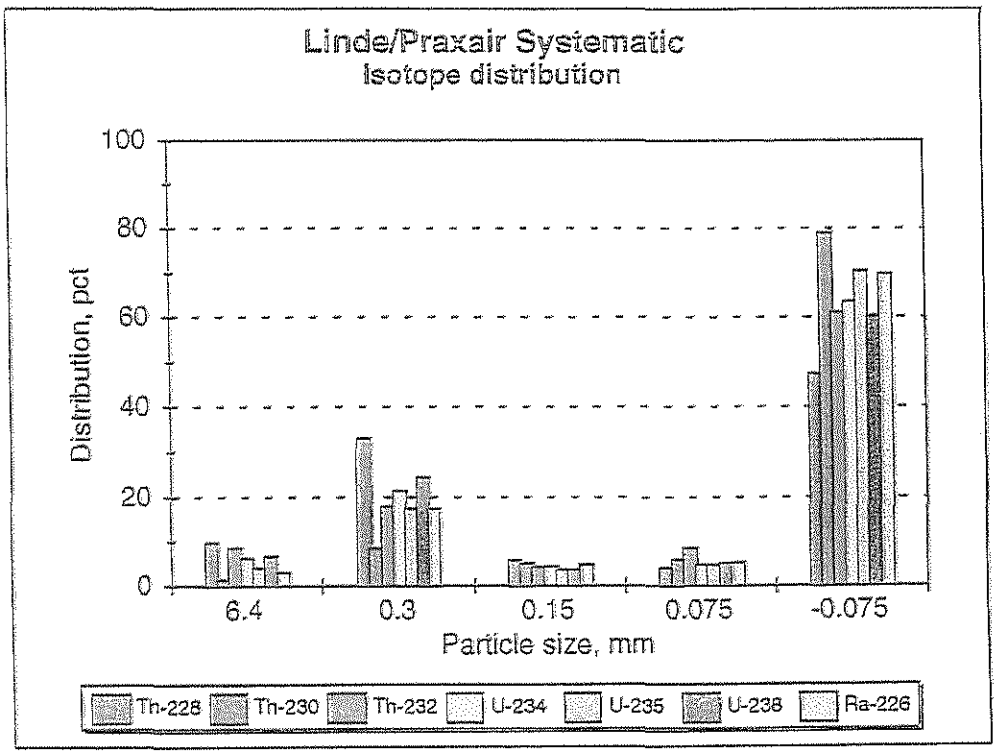

Figure 8. Particle size analysis, isotope analysis, and isotope distribution for Linde/Praxair systematic sample.

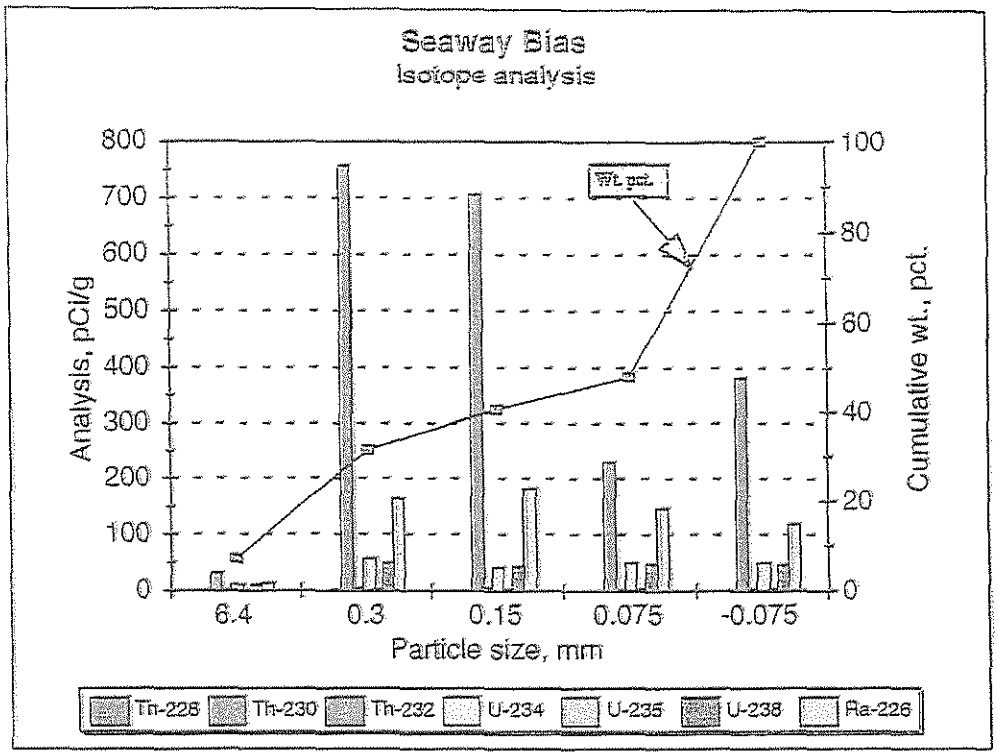

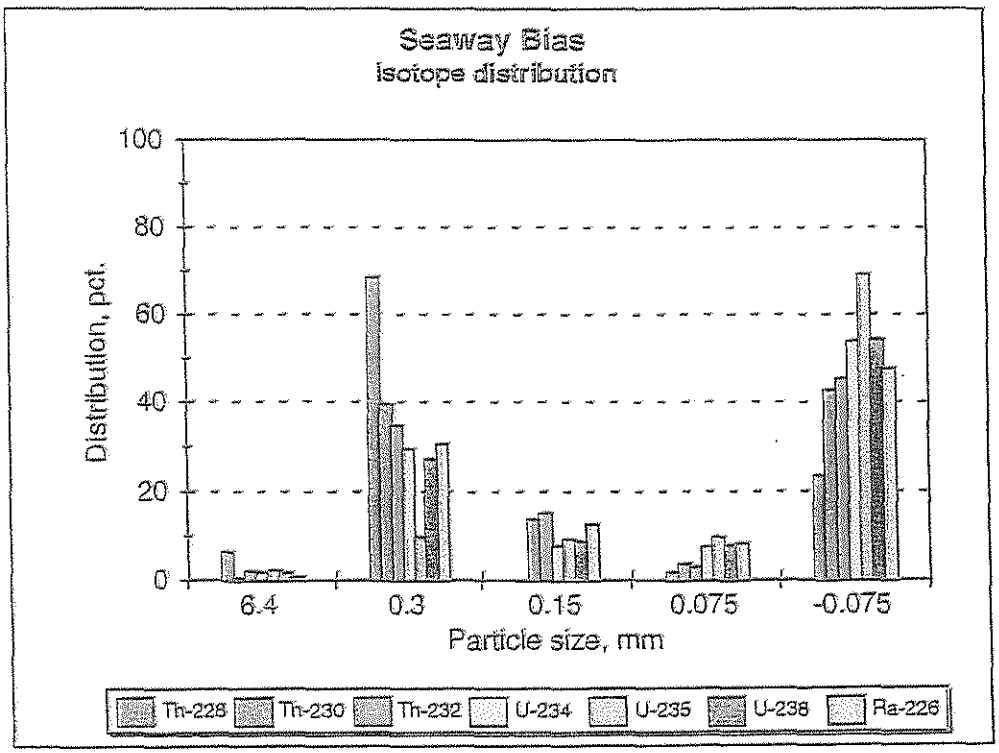

Figure 9. Particle size analysis, isotope analysis, and isotope distribution for Seaway bias sample.

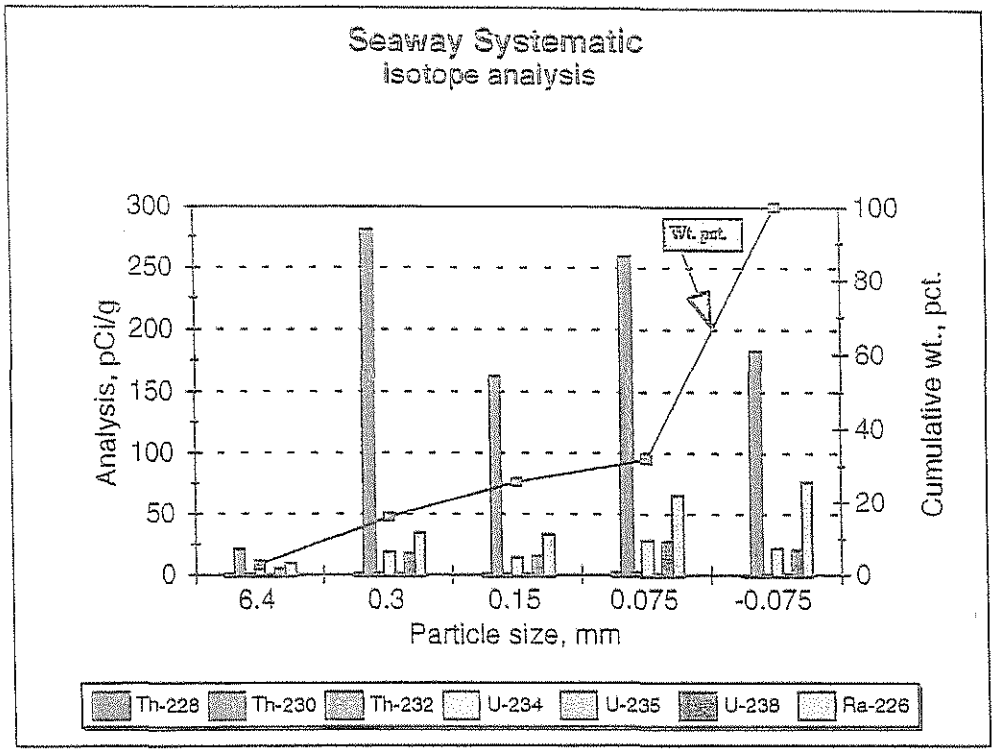

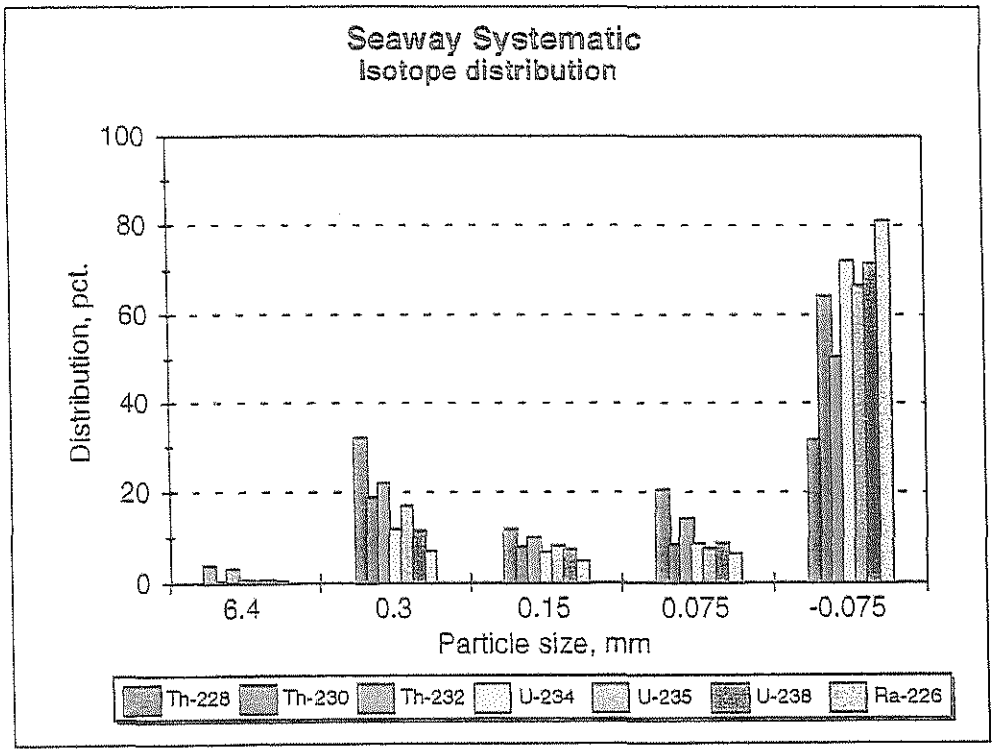

Figure 10. Particle size analysis, isotope analysis, and isotope distribution for Seaway systematic sample.

Mineralogy of samples

The weight distributions from heavy-liquid separation of the 0.3- by 0.15-mm and 0.15- by 0.075-mm size fractions are shown in table 17. The mineralogy of the size fractions of all eight samples is summarized by size fraction in tables 18 through 21.

Plus 6.4-mm size fractions. The plus 6.4-mm fractions of all eight samples consist of a mixture of rocks and man-made materials (table 18). The rocks include major amounts of limestone and chert, and small to trace amounts of sandstone, granite, gneiss, and basalt. Many of the rock fragments were eroded from concrete; these are more rounded than the native rocks and many have cement clinging to them. The man-made constituents include glassy, crystalline, and scoriaceous slags. Slags described as crystalline contain from 10 to 90 pct crystals (primarily melilite [$Ca_2(Mg,Al)(Al,Si)SiO_7$]) and dendritic inclusions of iron oxide. The scoriaceous slags appear much like volcanic cinders. Other man-made materials identified are small to trace amounts of concrete, brick, plastic, fiberglass, ceramic, and rusty iron.

Radiometric activity of the major constituents of the plus 6.4-mm fractions was estimated by isolating them and doing 5-minute counts with a scintillometer. By these estimates, the crystalline slags are most radioactive, followed by the glassy slags. Counts on natural rock fragments were indistinguishable from background counts using this technique.

Total slag comprises more than 50 pct of the Linde/Praxair and Ashland 1 and 2 systematic fractions, and the Ashland 1 and 2 bias fractions. The crystalline slag is most prominent in both Ashland 1 samples.

6.4- by 0.3-mm size fractions. The 6.4- by 0.3-mm fractions are composed of rocks, minerals, man-made constituents, and organic material (table 19). The most abundant rock types are limestone and chert, with minor amounts of sandstone, granitic rock, and siltstone. The most abundant minerals are quartz (SiO_2), calcite ($CaCO_3$), and feldspar ($KAlSi_3O_8$ and $(Na,Ca)Al(Al,Si)Si_2O_8$), with traces of opal ($SiO_2 \cdot nH_2O$), muscovite ($KAl_2(Si_3Al)O_{10}(OH,F)_2$), and amphibole-group minerals in some of the samples. Organic material (grasses, sticks, seeds, insect parts, snail shells) is ubiquitous but totals less than 10 pct in most samples. All except

those sample fractions from Linde/Praxair contain aggregates of clay and fine-grained carbonate minerals, hematite, and organic material that bind larger slag, mineral, and organic fragments together. These are termed "clay/carbonate aggregates" in tables 19 through 21, and comprise the majority of some sample fractions. Traces of a fine-grained, bright-colored (red, yellow, or green), layered material are associated with iron oxide in several of these samples; this may be a filter product.

The proportion of slag is different in each of these size fractions. Most fractions contain less than 10 pct slag, but the systematic fraction from the Linde/Praxair site.contains 60 to 90 pct slag. The proportion of slag in the bias fraction from this site is also elevated over other samples. The fractions from Linde/Praxair do not contain the fine-grained clay/carbonate aggregates that make up 15 to 80 pct of the other samples.

0.3- by 0.15-mm size fractions. The 0.3- by 0.15-mm fractions contain constituents similar to those in coarser fractions, with greater occurrence of individual mineral grains relative to rock fragments. Similarly, discrete melilite crystals present in this size fraction (table 20) probably were derived from coarser slag fragments. In each case, the higher percentage of material reports to the light fraction with specific gravity less than 2.90.

The heavy fractions of the systematic samples were separated into magnetic and nonmagnetic fractions with a hand magnet. The magnetic fractions consist of magnetite (Fe_3O_4), much of which is intergrown with ilmenite ($FeTiO_3$); oxide-coated metallic iron; entrained hematite (Fe_2O_3), goethite ($FeO(OH)$), and spheres of iron oxide; and traces of bright-colored (yellow, orange, or green) layered material similar to that seen associated with iron oxide in coarser fractions. Ferromagnesian silicate minerals (primarily amphibole-group minerals with some pyroxene-group minerals) are relatively abundant in the nonmagnetic portions of the heavy fractions. Small to trace amounts of other minerals, many of which were identified in the SEM study, were identified in one or more of the samples. These include garnet, zircon ($ZrSiO_4$), apatite ($Ca_5(PO_4)_3(F,Cl,OH)$), epidote ($Ca_2(Fe,Al)_3(SiO_4)_3(OH)$), chlorite, muscovite, magnesite ($MgCO_3$), sphene ($CaTiSiO_5$), pyrite (FeS_2), gypsum ($CaSO_4 \cdot 2H_2O$), tourmaline, rutile (TiO_2), monazite ($(La,Ce)PO_4$), leucoxene (an alteration product of ilmenite), and kyanite (Al_2SiO_5).

The 0.3- by 0.15-mm bias fractions were chosen for mounting, polishing, and detailed SEM study because these samples contain a larger amount of radioactive material. Examination by SEM showed that small amounts of uranium occur in both the heavy and light fractions, and primarily in man-made materials. Uranium compounds occur in the light fractions because small amounts are locked with low-density grains.

Slag fragments in both the light and heavy fractions contain blebs of uranium oxide compounds. Figure 11A shows a grain from the light fraction of the Linde/Praxair bias sample. Bright uranium-oxide compounds are locked with dark gray quartz in a medium-gray, glassy slag matrix. The slag is characterized by gas pores (black spheres in the matrix) and arc-shaped boundaries. Figure 11B shows a higher concentration of bright, aggregated spheres of uranium oxide locked in slag from the heavy fraction of the Seaway bias sample.

The heavy fraction of the Linde/Praxair bias sample contains what is presumed to be filter cake, that is contaminated with uranium oxide. Figure 12 shows an earthy, weakly banded grain (medium gray) at the right-center of the photomicrograph. It contains bright angular fragments of uranium oxide and subangular and subrounded dark gray quartz grains. Other grains in the figure are iron oxides, amphiboles, and slag.

Uranium particles are also agglomerated with slag fragments and minerals in clay/carbonate aggregates. Figure 13 shows such an aggregate from the Seaway bias light fraction. Some of the very small, bright particles are uranium compounds, and some are tin compounds. The darker matrix is clay and carbonate.

Ore fragments containing uraninite (UO_2) and other uranium minerals locked with gangue minerals are rare constituents of the Linde/Praxair heavy and light fractions. Figure 14 shows a calcium-uranium mineral (possibly zellerite, [$Ca(UO_2)(CO_3)_2 \cdot 5H_2O$]) as bright fragments locked in a medium gray grain of albite ($NaAlSi_3O_8$). Other uranium-oxide grains that may be ore fragments occur as blebs approximately 2 micrometers in largest dimension in iron oxide grains in the heavy fraction of the Ashland 2 sample.

Although isotopic analyses indicate that thorium is most abundant in the Seaway samples, thorium was not identified in any phases in any of the samples. Apatite and zircon are common hosts for thorium and uranium, but EDX analyses did not detect them in these minerals. Traces of hafnium are present in the apatite. The heavy portions of the Ashland 1 and 2 bias fractions contain traces of lead-bearing grains; many have metallic lead cores surrounded by lead oxide or carbonate and iron oxide compounds (fig. 15).

0.15- by 0.075-mm size fractions. The constituents of the 0.15- by 0.075-mm fractions of the eight samples are the same as in the 0.3- by 0.15-mm fractions (table 21). The Linde/Praxair systematic heavy sample and Ashland 1 systematic heavy sample contain more slag than the coarser fraction of the respective samples; the Linde/Praxair bias light sample, Seaway bias heavy sample, and Ashland 1 and 2 bias heavy samples contain less slag. The proportion of magnetic material remains approximately the same or decreases in all of the finer fractions.

Minus 0.075-mm size systematic fractions. Carbonate minerals were identified during petrographic examination of the systematic fractions, but made up less than 10 pct of each. Organic material was also present. These constituents were removed from the minus 0.075-mm systematic fractions to simplify and expedite XRD analysis.

XRD patterns were similar for all of the systematic fractions. The most abundant phase identified was quartz, with minor amounts of albite (plagioclase feldspar - $NaAlSi_3O_8$), and traces of muscovite and chamosite (a chlorite-group mineral). The peak intensities for each sample were somewhat less than would be expected for samples consisting only of these minerals. This indirectly suggests the presence of amorphous slag material.

No clay minerals were identified by XRD in these fractions. SEM-EDX elemental analyses of aggregates found in the coarser size fractions support the admixture of clay minerals and carbonate minerals in the fine-grained portions of the aggregates. One would expect that these clays would also be present in the finest size fractions. Although no clay minerals were identified by XRD, the poor filtering characteristics of these samples suggest that many of the constituents are probably clay-sized (<0.002 mm).

Figure 11 A. Uranium oxide compounds in slag fragments from 0.3- by 0.15-mm fraction of Linde/Praxair bias sample, light (S.G. < 2.90) material. Scale bar at bottom of SEM photomicrograph represents 100 micrometers.

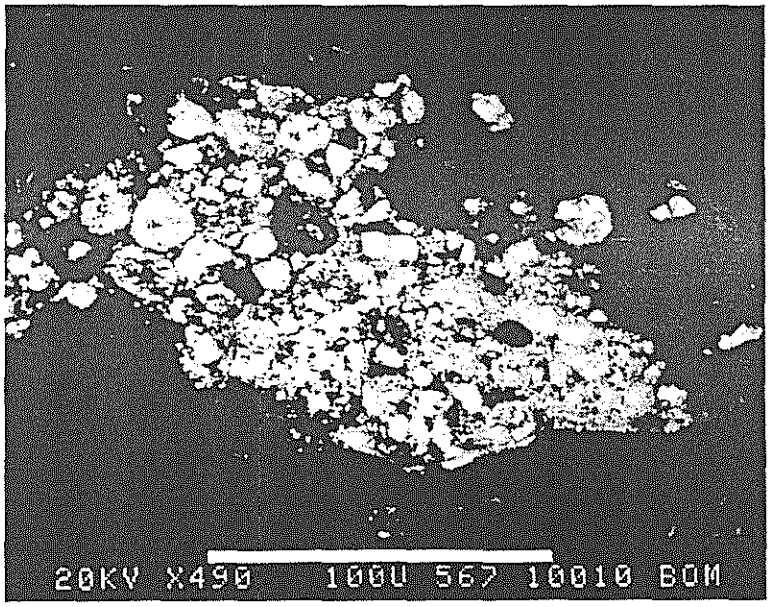

Figure 11 B. Uranium oxide compounds in slag fragments from 0.3- by 0.15-mm fraction of Seaway bias sample, heavy (S.G. > 2.90) material. Scale bar at bottom of SEM photomicrograph represents 100 micrometers.

Figure 12. Filter cake (multi-phased grain at center and to right of photomicrograph) containing uranium oxide compound. Rounded grains included in the same grain are probably silica. Some of the surrounding grains are iron oxides (medium to bright grains), an amphibole (platy elongated grain at left), and slag (grain at bottom of photo with patterned surface). From 0.3- by 0.15-mm fraction of Linde/Praxair bias sample, heavy (S.G. > 2.90) material. Width of field of SEM photomicrograph is approximately 0.5 mm.

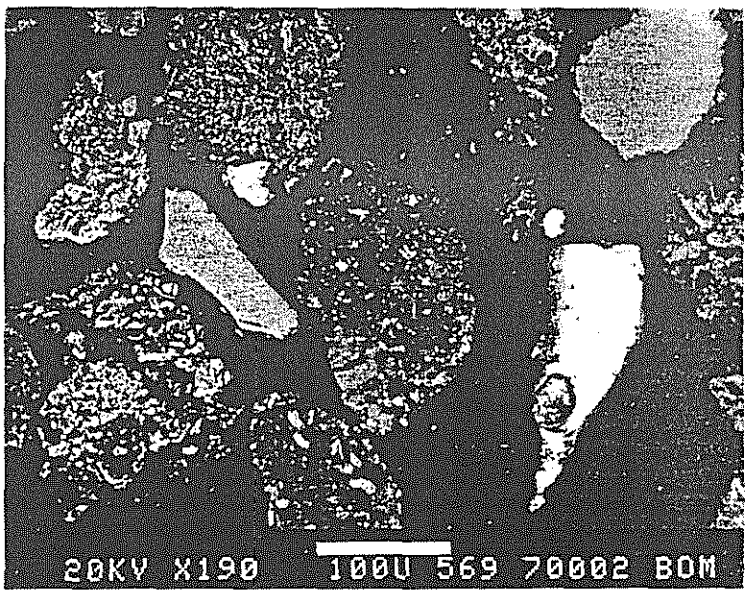

Figure 13. Clay/carbonate aggregates from the Seaway bias 0.3- by 0.15-mm fraction, light (S.G. < 2.90) material. Some of the bright particles enclosed within the central grain are uranium compounds. Others are tin compounds. Scale bar at bottom of SEM photomicrograph represents 100 micrometers.

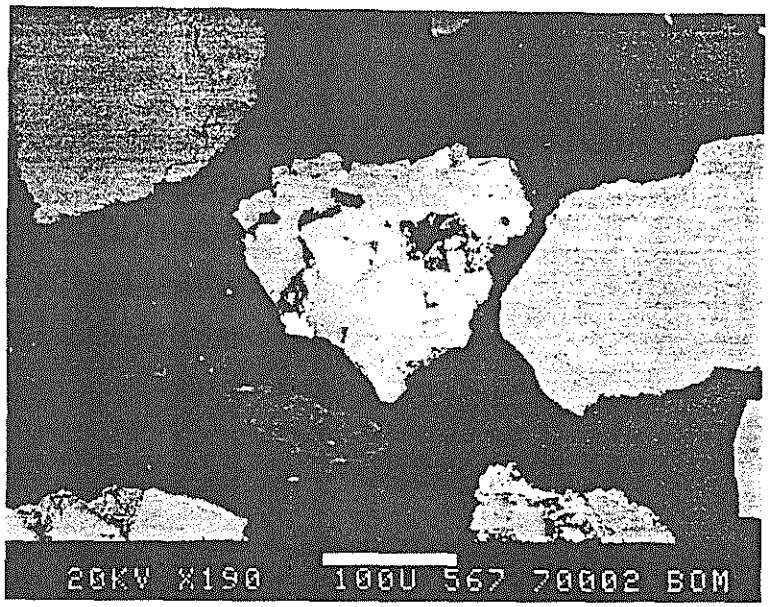

Figure 14. Calcium-uranium carbonate mineral (possibly zellerite [$Ca(UO_2)(CO_3)_2 \cdot 5H_2O$]) hosted by albite in the Linde/Praxair bias 0.3- by 0.15-mm fraction, light (S.G. < 2.90) material. Other materials are quartz (right and lower right of photo), organic fragment (bottom center, nearly as dark as matrix), and clay/carbonate aggregates (very bottom of photo). Scale bar at bottom of SEM photomicrograph represents 100 micrometers.

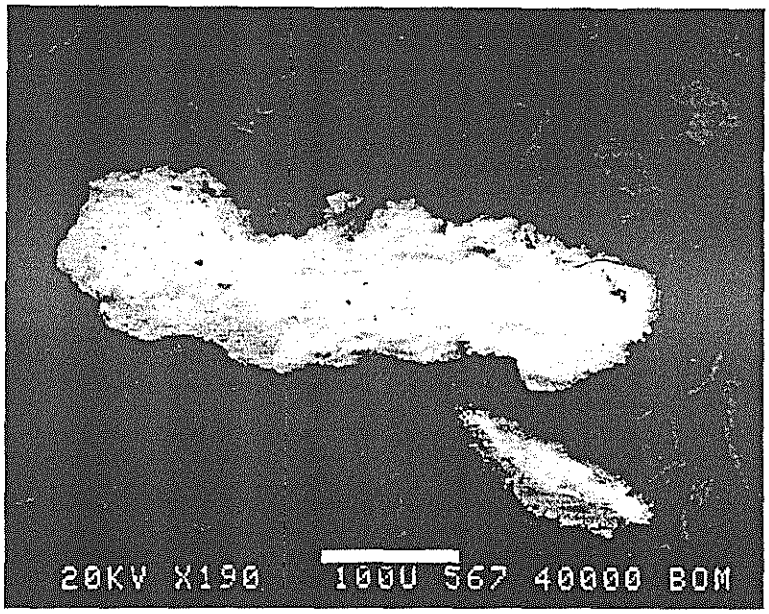

Figure 15. Grain of lead and iron oxides from Ashland 1 bias 0.3- by 0.15-mm fraction, heavy (S.G. > 2.90) material. Very bright streak through center of large grain is probably metallic lead. Next brightest portions of both grains are lead oxide or carbonate. Least bright portions are iron oxides. Small, elongate, bright fragments in epoxy matrix are remnants of sodium polytungstate compound used in heavy-liquid separation. Scale bar at bottom of SEM photomicrograph represents 100 micrometers.

Implications for cleaning the Tonawanda soils with mineral-processing technology

Conventional mineral-processing technology is unlikely to produce a significant fraction of clean soil (<5 pCi/g) in a volume-reduction strategy. The problem of particle liberation will adversely affect all physical separation techniques. Scrubbing followed by size separation would leave significant contamination in all size fractions because unliberated contaminated particles exist in all of the fractions. The results from heavy-liquid separation, an indication of the effectiveness of gravity separation, showed that contaminated particles report to both heavy and light fractions.

Low-intensity magnetic separation with a hand magnet was used in this study primarily as an aid to mineral identification in some of the size fractions, and magnetic and nonmagnetic products were produced. High-gradient magnetic separation has been used to concentrate uranium from ores with some success. Recoveries up to 95 pct have been reported but are often significantly less due to the effects of particle size, liberation, and other ore-specific properties, as well as to separator parameters such as magnetic field, matrix, and throughput.[5] The characteristics of the Tonawanda soils would likely result in low recoveries. The distribution of radioactive contamination throughout all of the size ranges investigated and the locked or entrained nature of the contaminants suggests magnetic separation would not effectively produce a clean soil fraction.

Selective leaching of these soils to remove contamination would also likely be ineffective. Some of the contamination is in porous iron oxides and in poorly cemented aggregates of clay and carbonate minerals (figs. 12 and 13). However, much of the contamination is locked within competent grains or glassy slag matrix (figs. 11 and 14), so leachant penetration would be difficult. The poor filtering characteristics of the fines suggests that solids-liquid separation would be a problem in either heap or vat leaching.

---

[5]Svoboda, J. Magnetic Methods for the Treatment of Minerals. Elsevier Science Publishers B.V., Amsterdam, The Netherlands, 1987.

CONCLUSIONS

The results of size and isotopic analyses and mineralogical characterization studies on soil samples from the Tonawanda site indicate that the soils are not amenable to conventional physical mineral-processing technologies to concentrate the radiation contamination in a volume-reduction strategy. Isotopic contaminants are distributed throughout all of the size fractions of the samples, and they are locked in host materials that would preclude efficient and effective separation.

Table 1. Tonawanda sample description.

ALRC No.	Location	Description	α-β count, cpm
3371	Linde/Praxair (129)	Bias, Area 3	>400
3372	Linde/Praxair (129)	Systematic, Areas 3+4	>200
3373	Seaway (123)	Bias, Area A	>400
3374	Seaway (123)	Systematic, Area A	~200
3375	Ashland 1 (103)	Bias	~900
3376	Ashland 1 (103)	Systematic	~200
3377	Ashland 2 (132)	Bias	~800
3378	Ashland 2 (132)	Systematic	~200

Table 2. Sample weights and moisture contents.

ALRC No.	Sample description	Weight, g		Weight of water, g (by difference)	Percent moisture, wt water/wt as rec'd
		As rec'd	Dry		
3371	Linde/Prax Bias	4779	4218	561	11.7
3372	Linde/Prax Sys.	4439	4033	406	9.1
3373	Seaway Bias	3414	2882	532	15.6
3374	Seaway Sys.	3672	3242	430	11.7
3375	Ashland 1 Bias	3671	2942	729	19.9
3376	Ashland 1 Sys.	4381	3715	666	15.2
3377	Ashland 2 Bias	4426	3732	694	15.7
3378	Ashland 2 Sys.	4825	4221	604	12.5

Table 3. Isotopic analysis of head samples.

	Analysis, pCi/g						
Sample	Th-228	Th-230	Th-232	U-234	U-235	U-238	Ra-226
Ashland 1 Bias	1.13 ± 0.8	<0.1	0.61 ± 0.07	160 ± 38	26.2 ± 6.3	175 ± 42	63.2 ± 10.5
Ashland 1 Sys.	1.58 ± 0.16	<0.1	1.25 ± 0.51	79.0 ± 11.7	3.15 ± 0.90	76.0 ± 11.3	17.3 ± 2.0
Ashland 2 Bias	<0.1	<0.1	0.55 ± 0.05	102 ± 21	6.2 ± 3.0	129 ± 27	33.0 ± 4.9
Ashland 2 Sys.	<0.1	<0.1	0.30 ± 0.3	123 ± 15	5.62 ± 1.04	123 ± 15	16.1 ± 1.7
Linde/Prax Bias	2.8 ± 1.9	269 ± 122	3.4 ± 2.2	222 ± 40	10.0 ± 5.4	233 ± 42	126 ± 2.4
Linde/Prax Sys.	1.3 ± 0.5	103 ± 19	2.0 ± 0.6	129 ± 21	8.5 ± 3.1	129 ± 21	98.9 ± 2.0
Seaway Bias	2.9 ± 0.2	1060 ± 296	6.2 ± 2.2	42.8 ± 9.4	5.2 ± 1.8	43.3 ± 9.5	158 ± 2.7
Seaway Sys.	3.7 ± 6.1	743 ± 843	7.5 ± 10.4	18.1 ± 5.5	4.1 ± 1.7	19.3 ± 5.8	62.0 ± 1.6

Table 4. Isotopic analysis of sized fractions separated from Ashland 1 samples.

Bias sample	Analysis, pCi/g						
Size fraction, mm	Th-228	Th-230	Th-232	U-234	U-235	U-238	Ra-226
Plus 6.4	0.71 ± 0.07	<0.1	1.28 ± 0.11	14.1 ± 3.4	0.56 ± 0.19	14.2 ± 3.4	6.08 ± 1.09
6.4 by 0.3	1.18 ± 0.08	<0.1	1.10 ± 0.11	105 ± 18	5.10 ± 2.89	125 ± 22	80.8 ± 12.8
0.3 by 0.15	0.86 ± 0.07	<0.1	1.52 ± 0.74	86.5 ± 3.3	5.06 ± 2.00	90 ± 4.0	101 ± 12
0.15 by 0.075	<0.1	<0.1	1.75 ± 0.10	138 ± 60	5.52 ± 1.36	174 ± 76	81.4 ± 9.4
Minus 0.075	0.86 ± 0.06	<0.1	0.50 ± 0.07	197 ± 53	8.91 ± 2.40	275 ± 74	54.6 ± 6.6

Systematic sample	Analysis, pCi/g						
Size fraction, mm	Th-228	Th-230	Th-232	U-234	U-235	U-238	Ra-226
Plus 6.4	0.71 ± 0.50	<0.1	0.56 ± 0.18	8.37 ± 1.71	0.36 ± 0.26	9.56 ± 1.90	1.56 ± 0.23
6.4 by 0.3	<0.1	<0.1	<0.1	159 ± 19	6.39 ± 1.16	161 ± 19	21.4 ± 3.1
0.3 by 0.15	<0.1	<0.1	0.63 ± 0.08	95.4 ± 3.7	4.4 ± 2.86	81.2 ± 3.1	43.3 ± 5.3
0.15 by 0.075	<0.1	<0.1	0.65 ± 0.10	64.5 ± 6.8	2.73 ± 0.55	64.4 ± 6.8	38.6 ± 5.7
Minus 0.075	<0.1	<0.1	0.88 ± 0.67	55.0 ± 5.3	2.54 ± 0.48	51.8 ± 5.0	22.8 ± 2.7

Table 5. Isotopic analysis of sized fractions separated from Ashland 2 samples.

Bias sample	Analysis, pCi/g						
Size fraction, mm	Th-228	Th-230	Th-232	U-234	U-235	U-238	Ra-226
Plus 6.4	0.66 ± 0.07	<0.1	2.1 ± 0.20	12.5 ± 5.6	0.75 ± 0.42	12.7 ± 5.8	8.19 ± 1.55
6.4 by 0.3	1.25 ± 0.46	<0.1	1.05 ± 0.11	110 ± 33	6.60 ± 2.05	103 ± 31	68.6 ± 10.9
0.3 by 0.15	1.09 ± 0.54	<0.1	1.39 ± 0.56	108 ± 24	5.95 ± 2.63	137 ± 31	67.8 ± 8.1
0.15 by 0.075	1.58 ± 0.90	<0.1	0.87 ± 0.13	8.49 ± 0.65	0.12 ± 0.10	9.23 ± 0.71	74.7 ± 8.7
Minus 0.075	1.04 ± 0.56	<0.1	2.38 ± 0.12	71.4 ± 1.6	3.09 ± 0.74	67.9 ± 1.5	26.4 ± 3.2

Systematic sample	Analysis, pCi/g						
Size fraction, mm	Th-228	Th-230	Th-232	U-234	U-235	U-238	Ra-226
Plus 6.4	<0.1	<0.1	0.41 ± 0.05	101 ± 9	4.13 ± 0.60	102 ± 9	0.67 ± 0.08
6.4 by 0.3	<0.1	<0.1	0.36 ± 0.05	52 ± 3.6	2.24 ± 0.29	52.3 ± 13.6	23.1 ± 2.8
0.3 by 0.15	<0.1	<0.1	0.50 ± 0.08	92.9 ± 9.3	3.37 ± 0.63	92.4 ± 9.2	30.3 ± 4.5
0.15 by 0.075	<0.1	<0.1	0.34 ± 0.04	156 ± 5	8.77 ± 4.03	154 ± 5	30.8 ± 3.6
Minus 0.075	<0.1	<0.1	0.30 ± 0.03	46.0 ± 5.0	1.84 ± 0.60	46.9 ± 6	16.9 ± 1.8

Table 6. Isotopic analysis of sized fractions separated from Linde/Praxair samples.

Bias sample	Analysis, pCi/g						
Size fraction, mm	Th-228	Th-230	Th-232	U-234	U-235	U-238	Ra-226
Plus 6.4	1.3 ± 0.6	6.2 ± 1.6	1.0 ± 0.5	28.9 ± 6.8	1.7 ± 1.1	25 ± 6.1	11.9 ± 0.8
6.4 by 0.3	1.0 ± 0.6	47.9 ± 12.2	1.9 ± 0.8	117 ± 20	3.5 ± 2.0	104 ± 18.2	60.4 ± 1.7
0.3 by 0.15	1.0 ± 0.5	142 ± 30.5	1.6 ± 0.6	172 ± 27.7	12 ± 4.0	166 ± 26.9	140 ± 2.6
0.15 by 0.075	2.2 ± 1.5	334 ± 140	2.2 ± 1.5	342 ± 60.0	9.6 ± 5.5	322 ± 56.8	234 ± 3.3
Minus 0.075	1.7 ± 1.0	337 ± 114	2.6 ± 1.4	452 ± 80.3	12.3 ± 6.7	483 ± 85	280 ± 3.6

Systematic sample	Analysis, pCi/g						
Size fraction, mm	Th-228	Th-230	Th-232	U-234	U-235	U-238	Ra-226
Plus 6.4	1.0 ± 0.4	17.3 ± 3.7	1.2 ± 0.5	84 ± 13.5	2.6 ± 1.3	84.6 ± 13.6	28.9 ± 1.1
6.4 by 0.3	1.2 ± 0.6	35.3 ± 7.4	0.9 ± 0.4	105 ± 17.5	4.1 ± 1.7	109 ± 18.1	58.2 ± 1.5
0.3 by 0.15	1.0 ± 0.8	100 ± 39.1	1.0 ± 0.8	102 ± 15.9	4.0 ± 1.5	76.3 ± 12.3	75.4 ± 1.7
0.15 by 0.075	0.9 ± 0.9	150 ± 68.1	2.6 ± 1.8	139 ± 24.8	6.7 ± 3.0	137 ± 24.4	105 ± 2.0
Minus 0.075	1.4 ± 1.4	266 ± 135	2.5 ± 2.0	253 ± 75.1	13.5 ± 12.8	219 ± 67.6	189 ± 2.7

Table 7. Isotopic analysis of sized fractions separated from Seaway samples.

Bias sample	Analysis, pCi/g						
Size fraction, mm	Th-228	Th-230	Th-232	U-234	U-235	U-238	Ra-226
Plus 6.4	0.8 ± 0.4	31.6 ± 6.5	0.9 ± 0.4	11.4 ± 2.1	0.6 ± 0.3	11.2 ± 2.1	14.1 ± 0.8
6.4 by 0.3	2.5 ± 3.0	757 ± 562	4.6 ± 4.6	57.8 ± 13.6	2.5 ± 1.6	50.6 ± 12.1	164 ± 2.8
0.3 by 0.15	ND	707 ± 695	5.4 ± 6.8	40.8 ± 7.6	2.0 ± 1.1	44.3 ± 8.1	182 ± 2.9
0.15 by 0.075	0.2 ± 0.4	230 ± 64.9	1.3 ± 0.7	48.7 ± 11.5	2.6 ± 1.6	48.2 ± 11.5	147 ± 2.6
Minus 0.075	0.4 ± 0.4	382 ± 124	2.8 ± 1.4	49.5 ± 8.1	2.6 ± 0.9	47 ± 7.7	119 ± 2.4

ND = Not detected.

Systematic sample	Analysis, pCi/g						
Size fraction, mm	Th-228	Th-230	Th-232	U-234	U-235	U-238	Ra-226
Plus 6.4	0.9 ± 0.4	21.2 ± 4.7	1.1 ± 0.5	4.9 ± 1.6	0.2 ± 0.2	5.0 ± 1.6	9.6 ± 0.6
6.4 by 0.3	1.6 ± 2.2	281 ± 185	1.6 ± 1.9	18.9 ± 3.5	1.2 ± 0.5	17.7 ± 3.3	34.6 ± 1.2
0.3 by 0.15	0.8 ± 0.8	162 ± 64.2	1.0 ± 0.8	14.5 ± 2.4	0.8 ± 0.4	15.5 ± 2.6	33.3 ± 1.1
0.15 by 0.075	2.1 ± 3.1	259 ± 229	2.1 ± 3.1	28.2 ± 4.7	1.1 ± 0.4	27.9 ± 4.7	65.6 ± 1.6
Minus 0.075	0.3 ± 0.7	183 ± 115	0.7 ± 1.1	21.9 ± 3.4	0.9 ± 0.4	20.9 ± 3.3	76.6 ± 1.7

Table 8. Isotopic analysis of wash-water samples from sizing procedure.

	Analysis, pCi/l				
Sample	**Th-228**	**Th-230**	**Th-232**	**Total U**	**Ra-226**
Ashland 1 Bias	<0.6	1.09 ± 0.45	<0.6	269	3.0 ± 2.8
Ashland 1 Sys.	<0.6	<0.6	<0.6	60	<0.6
Ashland 2 Bias	<0.6	1.10 ± 0.77	<0.6	366	2.6 ± 0.6
Ashland 2 Sys.	<0.6	<0.6	<0.6	113	<0.6
Linde/Prax Bias	<1.0	1.4 ± 0.7	<0.9	668	1.9 ± 0.5
Linde/Prax Sys.	<2.0	1.8 ± 1.2	<2.2	493	2.3 ± 0.5
Seaway Bias	<2.8	1.5 ± 0.8	<1.2	37.3	3.0 ± 0.6
Seaway Sys.	<2.5	0.7 ± 0.7	<2.2	38	1.0 ± 0.4

Table 9. Particle size analysis, isotope analysis, and distribution for Ashland 1 bias sample.

	Particle size analysis			Isotope analysis, pCi/g						
ALRC No.	Size fraction, mm	Wt. %	Cum wt%	Th-228	Th-230	Th-232	U-234	U-235	U-238	Ra-226
3375.2	Plus 6.4	7.3	7.3	0.71	<0.1	1.28	14.1	0.56	14.2	6.08
3375.3	6.4 by 0.3	17.6	24.9	1.18	<0.1	1.1	105	5.1	125	80.8
3375.4	0.3 by 0.15	7.4	32.3	0.86	<0.1	1.52	86.5	5.06	90	101
3375.5	0.15 by 0.075	7.2	39.5	<0.1	<0.1	1.75	138	5.52	174	81.4
3375.6	Minus 0.075	60.5	100	0.86	<0.1	0.5	197	8.9	275	54.6
Calculated head		100		0.84	<0.1	0.82	155	7.09	208	61
Head analysis				1.13	<0.1	0.61	160	26.2	175	63.2

				Distribution, pct.						
3375.2	Plus 6.4	7.3	7.3	6.1	0	11.3	0.7	0.6	0.5	0.7
3375.3	6.4 by 0.3	17.6	24.9	24.6	0	23.3	11.9	12.6	10.5	23.3
3375.4	0.3 by 0.15	7.4	32.3	7.6	0	13.6	4.1	5.3	3.2	12.3
3375.5	0.15 by 0.075	7.2	39.5	0	0	15.2	6.4	5.6	6	9.6
3375.6	Minus 0.075	60.5	100	61.7	0	36.6	76.9	75.9	79.8	54.1
Total		100		100	0	100	100	100	100	100

Table 10. Particle size analysis, isotope analysis, and distribution for Ashland 1 systematic sample.

	Particle size analysis			Isotope analysis, pCi/g						
ALRC No.	Size fraction, mm	Wt. %	Cum wt%	Th-228	Th-230	Th-232	U-234	U-235	U-238	Ra-226
3376.2	Plus 6.4	16	16	0.71	<0.1	0.56	8.37	0.36	9.56	1.56
3376.3	6.4 by 0.3	15.2	31.2	<0.1	<0.1	<0.1	159	6.39	161	21.4
3376.4	0.3 by 0.15	7.1	38.3	<0.1	<0.1	0.63	95.4	4.4	81.2	43.3
3376.5	0.15 by 0.075	5.9	44.2	<0.1	<0.1	0.65	64.5	2.73	64.4	38.6
3376.6	Minus 0.075	55.8	100	<0.1	<0.1	0.88	55	2.54	51.8	22.8
Calculated head		100		0.11	<0.1	0.66	66.8	2.91	64.5	21.6
Head analysis				1.13	<0.1	0.61	160	26.2	175	63.2

				Distribution, pct.						
3376.2	Plus 6.4	16	16	100	0	13.5	2	2	2.4	1.1
3376.3	6.4 by 0.3	15.2	31.2	0	0	0	36.1	33.2	37.9	15.1
3376.4	0.3 by 0.15	7.1	38.3	0	0	6.7	10.2	10.7	8.9	14.2
3376.5	0.15 by 0.075	5.9	44.2	0	0	5.8	5.7	5.5	5.9	10.6
3376.6	Minus 0.075	55.8	100	0	0	74	46	48.6	44.9	59
Total		100		100	0	100	100	100	100	100

Table 11. Particle size analysis, isotope analysis, and distribution for Ashland 2 bias sample.

	Particle size analysis			Isotope analysis, pCi/g						
ALRC No.	Size fraction, mm	Wt. %	Cum wt%	Th-228	Th-230	Th-232	U-234	U-235	U-238	Ra-226
3377.2	Plus 6.4	3.7	3.7	0.66	<0.1	2.1	12.5	0.75	12.7	8.19
3377.3	6.4 by 0.3	13.6	17.3	1.25	<0.1	1.05	110	6.6	103	68.6
3377.4	0.3 by 0.15	7.6	24.9	1.09	<0.1	1.39	108	5.95	137	67.8
3377.5	0.15 by 0.075	6.4	31.3	1.58	<0.1	0.87	8.49	0.12	9.23	74.7
3377.6	Minus 0.075	68.7	100	1.04	<0.1	2.38	71.4	3.09	67.9	26.4
Calculated head		100		1.09	<0.1	2.01	73.2	3.5	72.1	37.7
Head analysis				<0.1	<0.1	0.55	102	6.2	129	33

				Distribution, pct.						
3377.2	Plus 6.4	3.7	3.7	2.2	0	3.8	0.6	0.8	0.7	0.8
3377.3	6.4 by 0.3	13.6	17.3	15.6	0	7.1	20.5	25.6	19.4	24.8
3377.4	0.3 by 0.15	7.6	24.9	7.6	0	5.2	11.2	12.9	14.4	13.6
3377.5	0.15 by 0.075	6.4	31.3	9.2	0	2.8	0.7	0.2	0.8	12.7
3377.6	Minus 0.075	68.7	100	65.4	0	81.1	67	60.5	64.7	48.1
Total		100		100	0	100	100	100	100	100

Table 12. Particle size analysis, isotope analysis, and distribution for Ashland 2 systematic sample.

	Particle size analysis			Isotope analysis, pCi/g						
ALRC No.	Size fraction, mm	Wt. %	Cum wt%	Th-228	Th-230	Th-232	U-234	U-235	U-238	Ra-226
3378.2	Plus 6.4	4.4	4.4	<0.1	<0.1	0.41	101	4.13	102	0.67
3378.3	6.4 by 0.3	14	18.4	<0.1	<0.1	0.36	52	2.24	52.3	23.1
3378.4	0.3 by 0.15	7.6	26	<0.1	<0.1	0.5	92.9	3.37	92.4	30.3
3378.5	0.15 by 0.075	6.6	32.6	<0.1	<0.1	0.34	156	8.77	154	30.8
3378.6	Minus 0.075	67.4	100	<0.1	<0.1	0.3	46	1.84	46.9	16.9
Calculated head		100		<0.1	<0.1	0.3	60	2.6	60.6	19
Head analysis				<0.1	<0.1	0.3	123	5.62	123	16.1

				Distribution, pct.						
3378.2	Plus 6.4	4.4	4.4	0	0	5.4	7.3	7	7.3	0.2
3378.3	6.4 by 0.3	14	18.4	0	0	15.2	12.1	12.2	12	17
3378.4	0.3 by 0.15	7.6	26	0	0	11.5	11.8	10	11.6	12.1
3378.5	0.15 by 0.075	6.6	32.6	0	0	6.8	17.2	22.6	16.9	10.7
3378.6	Minus 0.075	67.4	100	0	0	61.1	51.6	48.2	52.2	60
Total		100		0	0	100	100	100	100	100

Table 13. Particle size analysis, isotope analysis, and distribution for Linde/Praxair bias sample.

	Particle size analysis			Isotope analysis, pCi/g						
ALRC No.	Size fraction, mm	Wt. %	Cum wt%	Th-228	Th-230	Th-232	U-234	U-235	U-238	Ra-226
3371.2	Plus 6.4	20.2	20.2	1.3	6.2	1	28.9	1.7	25	11.9
3371.3	6.4 by 0.3	24.7	44.9	1	47.9	1.9	117	3.5	104	60.4
3371.4	0.3 by 0.15	6.3	51.2	1	142	1.6	172	12	166	140
3371.5	0.15 by 0.075	4.8	56	2.2	334	2.2	342	9.6	322	234
3371.6	Minus 0.075	44	100	1.7	337	2.6	452	12.3	483	280
Calculated head		100		1.43	186	2	261	7.8	269	153
Head analysis				2.8	269	2.2	222	10	233	126

				Distribution, pct.						
3371.2	Plus 6.4	20.2	20.2	18.4	0.7	10	2.2	4.4	1.9	1.5
3371.3	6.4 by 0.3	24.7	44.9	17.3	6.4	23.2	11.1	11	9.5	9.3
3371.4	0.3 by 0.15	6.3	51.2	4.4	4.8	5	4.1	9.6	5.8	5.5
3371.5	0.15 by 0.075	4.8	56	7.4	8.6	5.2	6.3	5.9	3.9	7
3371.6	Minus 0.075	44	100	52.5	79.5	56.6	76.2	69.1	78.9	76.7
Total		100		100	100	100	100	100	100	100

Table 14. Particle size analysis, isotope analysis, and distribution for Linde/Praxair systematic sample.

	Particle size analysis			Isotope analysis, pCi/g						
ALRC No.	Size fraction, mm	Wt. %	Cum wt%	Th-228	Th-230	Th-232	U-234	U-235	U-238	Ra-226
3372.2	Plus 6.4	12.1	12.1	1	17.3	1.2	84	2.6	84.6	28.9
3372.3	6.4 by 0.3	33.8	45.9	1.2	35.3	0.9	105	4.1	109	58.2
3372.4	0.3 by 0.15	7	52.9	1	100	1	102	4	76.3	75.4
3372.5	0.15 by 0.075	5.6	58.5	0.9	150	2.6	139	6.7	137	105
3372.6	Minus 0.075	41.5	100	1.4	266	2.5	253	13.5	219	189
Calculated head		100		1.22	140	1.7	166	7.9	151	113
Head analysis				1.3	103	2	129	8.5	129	98.9

				Distribution, pct.						
3372.2	Plus 6.4	12.1	12.1	9.9	1.5	8.5	6.1	4	6.8	3.1
3372.3	6.4 by 0.3	33.8	45.9	33	8.5	17.9	21.5	17.4	24.4	17.5
3372.4	0.3 by 0.15	7	52.9	5.7	5	4.1	4.3	3.5	3.6	4.7
3372.5	0.15 by 0.075	5.6	58.5	4.1	6	8.5	4.7	4.7	5	5.1
3372.6	Minus 0.075	41.5	100	47.3	79	61	63.4	70.4	60.2	69.6
Total		100		100	100	100	100	100	100	100

Table 15. Particle size analysis, isotope analysis, and distribution for Seaway bias sample.

	Particle size analysis			Isotope analysis, pCi/g						
ALRC No.	Size fraction, mm	,Wt. %	Cum wt%	Th-228	Th-230	Th-232	U-234	U-235	U-238	Ra-226
3373.2	Plus 6.4	7.1	7.1	0.8	31.6	0.9	11.4	0.6	11.2	14.1
3373.3	6.4 by 0.3	24.4	31.4	2.5	757	4.6	57.8	2.5	50.6	164
3373.4	0.3 by 0.15	9.1	40.5	ND	707	5.4	40.8	2	44.3	182
3373.5	0.15 by 0.075	7.3	47.9	0.2	230	1.3	48.7	2.6	48.2	147
3373.6	Minus 0.075	52.1	100	0.4	382	2.8	49.5	2.6	47	119
Calculated head		100		0.9	467	3.2	47.9	2	45.2	130
Head analysis				2.9	1060	6.2	42.8	5.2	43.3	158

				Distribution, pct.						
3373.2	Plus 6.4	7.1	7.1	6.4	0.5	2	1.7	2.2	1.8	0.8
3373.3	6.4 by 0.3	24.4	31.4	68.6	39.5	34.8	29.4	9.7	27.3	30.7
3373.4	0.3 by 0.15	9.1	40.5	0	13.8	15.2	7.7	9.3	8.9	12.7
3373.5	0.15 by 0.075	7.3	47.9	1.6	3.6	2.9	7.4	9.7	7.8	8.2
3373.6	Minus 0.075	52.1	100	23.4	42.6	45.1	53.8	69.1	54.2	47.6
Total		100		100	100	100	100	100	100	100

Table 16. Particle size analysis, isotope analysis, and distribution for Seaway systematic sample.

	Particle size analysis			Isotope analysis, pCi/g						
ALRC No.	Size fraction, mm	Wt. %	Cum wt%	Th-228	Th-230	Th-232	U-234	U-235	U-238	Ra-226
3374.2	Plus 6.4	2.8	2.8	0.9	21.2	1.1	4.9	0.2	5	9.6
3374.3	6.4 by 0.3	13	15.8	1.6	281	1.6	18.9	1.2	17.7	34.6
3374.4	0.3 by 0.15	9.6	25.4	0.8	162	1	14.5	0.8	15.5	33.3
3374.5	0.15 by 0.075	6.3	31.7	2.1	259	2.1	28.2	1.1	27.9	65.6
3374.6	Minus 0.075	68.3	100	0.3	183	0.7	21.9	0.9	20.9	76.6
Calculated head		100		0.6	194	0.9	20.7	0.9	19.9	64.4
Head analysis				3.7	743	7.5	18.1	4.1	19.3	62

				Distribution, pct.						
3374.2	Plus 6.4	2.8	2.8	3.9	0.3	3.3	0.7	0.6	0.7	0.4
3374.3	6.4 by 0.3	13	15.8	32.1	18.8	22	11.9	16.9	11.5	7
3374.4	0.3 by 0.15	9.6	25.4	11.8	8	10.1	6.7	8.3	7.4	4.9
3374.5	0.15 by 0.075	6.3	31.7	20.6	8.5	14.1	8.6	7.6	8.9	6.5
3374.6	Minus 0.075	68.3	100	31.6	64.4	50.5	72.1	66.6	71.5	81.2
Total		100		100	100	100	100	100	100	100

Table 17. Results of heavy-liquid separation at specific gravity 2.90 ± 0.02.

		Linde/Praxair	Seaway	Ashland 1	Ashland 2
Bias samples		**Weight, pct**			
0.3 by 0.15 mm	**Heavy**	11	3	5	2
	Light	90	97	95	98
	Total	100	100	100	100
0.15 by 0.075 mm	**Heavy**	13	3	8	3
	Light	87	97	92	97
	Total	100	100	100	100
Systematic samples					
0.3 by 0.15 mm	**Heavy**	9	1	2	1
	Light	91	99	98	99
	Total	100	100	100	100
0.15 by 0.075 mm	**Heavy**	18	5	5	4
	Light	82	95	95	96
	Total	100	100	100	100

Table 18. Composition, in pct of grain count, of plus 6.4-mm fractions; done by binocular microscope.[1]

	Systematic					Bias			
Constituent	L/P	Seaway	Ashland 1	Ashland 2		L/P	Seaway	Ashland 1	Ashland 2
Quartz/sandstone	5	11	1	6		1	12	1	7
Limestone	11	26	15	33		45	31	16	7
Chert	1		2	1		16	7		2
Clay/carbonate aggregates	6	3	1					1	
Slag - crystalline	22	25	52	28		31	20	63	25
Slag - scoriaceous	35	14	15	15		Tr.	15	6	16
Slag - glassy	12		11	10		4	3	4	25
Slag - mixed	4		1	1		1			
Iron oxide	3	1	1				8	1	2
Organics	1						1	1	
Other		20	1	6		2	3	7	16
Total	100	100	100	100		100	100	100	100

Tr. = Trace.
[1]May not be statistically representative.

Table 19. Composition, in pct of grain count, of 6.4-mm by 0.3-mm fractions; done by binocular microscope.[1]

	Systematic					Bias			
Constituent	L/P	Seaway	Ashland 1	Ashland 2		L/P	Seaway	Ashland 1	Ashland 2
Quartz/sand-stone/feldspar	5-10	25-35	3-5	35-40		40-50	3-5	8-10	10-12
Limestone/ calcite	2-4	1-2	<1	<1		10-15	<1	2-3	1-2
Chert	1-2					<1			
Clay/carbonate aggregates		15-20	70-90	50-60			80-100	70-80	65-75
Slag - all varieties	60-90	15-20	6-10	1-2		30-40	1-2	5-10	5-8
Iron oxide	8-12	<1	<1	<1		2-3		<1	<1
Organic	3-5	20-30	5-7	2-3		1-2	3-4	4-5	2-4
Other	<1	2-5	3-5	<1		<1	<1	<1	3-4
Total	79-124	78-113	87-119	88-108		83-112	88-113	87-110	86-106

[1]May not be statistically representative.

Table 20. Composition, in pct of grain count, of 0.3- by 0.15-mm fractions.

Systematic samples[1]	Linde/Praxair		Seaway		Ashland 1		Ashland 2	
Constituent	Lt.	Hvy.	Lt.	Hvy.	Lt.	Hvy.	Lt.	Hvy.
Quartz/feldspar/carbonate/chert	11	Tr.	32	9	8	1	23	3
Clay/carbonate aggregates	27	Tr.	43	2	61	3	63	5
Amphibole		1	Tr.	12		13		20
Garnet		Tr.		13		4		3
Slag - crystalline	39	1	2	9	5	14	1	4
Slag - glassy	1	Tr.	1		1	3		8
Hand-magnetic fraction		74		38		45		39
Iron oxide	6	20		6		13		11
Opaque	14	2	6	7	12	3	6	3
Organic	2	Tr.	14	Tr.	13		6	
Other		2	2	4		1	1	4
Total	100	100	100	100	100	100	100	100

Tr. = Trace.
[1]Done by binocular and petrographic microscopes.

Bias samples[2]	Linde/Praxair		Seaway		Ashland 1		Ashland 2	
Constituent	Lt.	Hvy.	Lt.	Hvy.	Lt.	Hvy.	Lt.	Hvy.
Quartz/feldspar/carbonate/chert	50-60	3	20-30	3	15-20	2	15-20	6
Clay/carbonate aggregates	5-15	3	60-70	4	55-65	13	70-75	12
Amphibole		9		13		6		18
Garnet		7				1		4
Slag and melilite	30-40	48	5-10	22	3-4	23	3-4	19
Iron oxide and iron		26		52	<1	49		32
Ilmenite plus magnetite		2		1				3
Organic					10-15	3	8-10	1
Other		2		5	5-7	3	<1	5
Total	85-115	100	85-110	100	88-112	100	96-110	100

[2]Done by reflected-light microscope and SEM.

Table 21. Composition, in pct of grain count, of 0.15- by 0.075-mm fractions; done by petrographic microscope.

Systematic samples	Linde/Praxair		Seaway		Ashland 1		Ashland 2	
Constituent	Lt.	Hvy.	Lt.	Hvy.	Lt.	Hvy.	Lt.	Hvy.
Quartz/feldspar/carbonate/chert	23	6	37	6	26	1	51	5
Clay/carbonate aggregates	15	5	20	2	46	2	31	4
Amphibole		2		20		8	Tr.	24
Garnet		Tr.		2		1		2
Slag - crystalline	27	33	1	5	4	37	3	8
Slag - glassy	4	3	3	4	3	4	1	4
Hand-magnetic fraction		37		38		31		27
Iron oxide	10	9	1	10	1	11		16
Opaque	17	3	12	4	12	2	7	4
Organic	3	1	26	1	8	Tr.	2	1
Other	1	1	Tr.	8	Tr.	3	5	5
Total	100	100	100	100	100	100	100	100

Tr. = Trace.

Bias samples	Linde/Praxair		Seaway		Ashland 1		Ashland 2	
Constituent	Lt.	Hvy.	Lt.	Hvy.	Lt.	Hvy.	Lt.	Hvy.
Quartz/feldspar/carbonate	23	Tr.	19	1	23	Tr.	19	1
Clay/carbonate aggregates	22	4	65	4	44	5	54	7
Amphibole		7	Tr.	20		4		26
Garnet		1		3				1
Slag - crystalline	20	47	1	2	4	13	3	9
Slag - glassy	1	3	1	2	2	1	1	3
Hand-magnetic fraction		27		47		32		29
Iron oxide	12	8	3	10	6	42	2	16
Opaque	17	3	6	6	13	3	11	7
Organic	5	Tr.	5	Tr.	8	Tr.	10	Tr.
Other		Tr.		5	Tr.			1
Total	100	100	100	100	100	100	100	100

Tr. = Trace.